We are IntechOpen, the world's leading publisher of Open Access books Built by scientists, for scientists

6,900
Open access books available

185,000
International authors and editors

200M
Downloads

154
Countries delivered to

Our authors are among the

TOP 1%
most cited scientists

12.2%
Contributors from top 500 universities

CLARIVATE ANALYTICS

BOOK CITATION INDEX

INDEXED

WEB OF SCIENCE™

Selection of our books indexed in the Book Citation Index
in Web of Science™ Core Collection (BKCI)

Interested in publishing with us?
Contact book.department@intechopen.com

Injection and Optical Spectroscopy of Localized States in II-VI Semiconductor Films

Denys Kurbatov, Anatoliy Opanasyuk and Halyna Khlyap

Additional information is available at the end of the chapter

http://dx.doi.org/10.5772/48290

1. Introduction

Novel achievements of nano- and microelectronics are closely connected with working-out of new semiconductor materials. Among them the compounds II-VI (where A = Cd, Zn, Hg and B = O, S, Se, Te) are of special interest. Due to unique physical properties these materials are applicable for design of optical, acoustical, electronic, optoelectronic and nuclear and other devices [1-3]. First of all the chalcogenide compounds are direct gap semiconductors where the gap value belongs to interval from 0.01 eV (mercury chalcogenides) up to 3.72 eV (ZnS with zinc blende crystalline structure) As potential active elements of optoelectronics they allow overlapping the spectral range from 0.3 μm to tens μm if using them as photodetectors and sources of coherent and incoherent light. The crystalline structure of II-VI compounds is cubic and hexagonal without the center of symmetry is a good condition for appearing strong piezoeffect. Crystals with the hexagonal structure have also pyroelectric properties. This feature may be used for designing acoustoelectronic devices, amplifiers, active delay lines, detectors, tensile sensors, etc. [1-2]. Large density of some semiconductors (CdTe, ZnTe, CdSe) makes them suitable for detectors of hard radiation and α–particles flow [4-5]. The mutual solubility is also important property of these materials. Their solid solutions give possibility to design new structures with in-advance defined gap value and parameters of the crystalline lattice, transmission region, etc. [6].

Poly- and monocrystalline films of II-VI semiconductors are belonging to leaders in field of scientific interest during the last decades because of possibility of constructing numerous devices of opto-, photo-, acoustoelectronics and solar cells and modules [2-5]. However, there are also challenges the scientists are faced due to structural peculiarities of thin chalcogenide layers which are determining their electro-physical and optical characteristics. The basic requirements for structure of thin films suitable for manufacturing various microelectronic devices are as follows: preparing stoichiometric single phase

monocrystalline layers or columnar strongly textured polycrystalline layers with low concentration of stacking faults (SF), dislocations, twins with governed ensemble of point defects (PD) [7-8]. However, an enormous number of publications points out the following features of these films: tend to departure of stioichiometric composition, co-existing two polymorph modifications (sphalerite and wurtzite), lamination morphology of crystalline grains (alternation of cubic and hexagonal phases), high concentration of twins and SF, high level of micro- and macrostresses, tend to formation of anomalous axial structures, etc. [2-3, 9]. Presence of different defects which are recombination centers and deep traps does not improve electro-physical and optical characteristics of chalcogenide layers. It restricts the application of the binary films as detector material, basic layers of solar energy photoconvertors, etc.

Thus, the problem of manufacturing chalcogenide films with controllable properties for device construction is basically closed to the governing of their defect structure investigated in detail. We will limit our work to the description of results from the examination of parameters of localized states (LS) in polycrystalline films CdTe, ZnS, ZnTe by the methods of injection and optical spectroscopy.

1.1. Defect classification in layers of II-VI compounds

Defects' presence (in the most cases the defects of the structure are charged) is an important factor affecting structure-depended properties of II-VI compounds [3, 5, 10]. Defects of the crystalline structure are commonly PD, 1-, 2-, and 3-dimensional ones [11-12]. Vacancies (V_A, V_B), interstitial atoms (A_i, B_i), antistructural defects (A_B, B_A), impurity atoms located in the lattice sites (C_A, C_B) and in the intersites (C_i) of the lattice are defects of the first type. However, the antistructural defects are not typical for wide gap materials (except CdTe) and they appear mostly after ionizing irradiation [13-14]. The PD in chalcogenides can be one- or two-charged. Each charged native defect forms LS in the gap of the semiconductor, the energy of the LS is ΔE_i either near the conduction band (the defect is a donor) or near the valence band (then the defect is an acceptor) as well as LS formed in energy depth are appearing as traps for charge carriers or recombination centers [15-16]. Corresponding levels in the gap are called shallow or deep LS. If the extensive defects are minimized the structure-depending properties of chalcogenides are principally defined by their PD. The effect of traps and recombination centers on electrical characteristics of the semiconductor materials is considered in [16]. We have to note that despite a numerous amount of publications about PD in Zn-Cd chalcogenides there is no unified theory concerning the nature of electrically active defects for the range of chalcogenide vapor high pressures as well as for the interval of high vapor pressure of chalcogen [13-14, 17-18].

Screw and edge dislocations are defects of second type they can be localized in the bulk of the crystalites or they form low-angled boundaries of regions of coherent scattering (RCS). Grain boundaries, twins and surfaces of crystals and films are defects of the third type. Pores and precipitates are of the 4th type of defects. All defects listed above are sufficiently

influencing on physical characteristics of the real crystals and films of II-VI compounds due to formation of LS (along with the PD) in the gap of different energy levels [17-20].

2. Using injection spectroscopy for determining parameters of localized states in II-VI compounds

2.1. Theoretical background of the injection spectroscopy method

The LS in the gap of the semiconductor make important contribution to the function of the device manufactured from the material solar cells, phodetectors, γ-ray detectors and others), for example, carriers' lifetime, length of the free path, etc., thus making their examination one of them most important problems of the semiconductor material science [3-5, 8, 13, 14, 18].

There are various methods for investigation of the energy position (E_t), concentration (N_t) and the energy distribution of the LS [21-23]. However, their applicability is restricted by the resistance of the semiconductors, and almost all techniques are suitable for low-resistant semiconductors. At the investigation of the wide gap materials II-VI the analysis of current-voltage characteristics (CVC) at the mode of the space-charge limited current (SCLC) had appeared as a reliable tool [24-25]. The comparison of experimental and theoretical CVCs is carried out for different trap distribution: discrete, uniform, exponential, double-exponential, Gaussian and others [26-36]. This method is a so-called direct task of the experiment and gives undesirable errors due to in-advance defined type of the LS distribution model used in further working-out of the experimental data. The information obtained is sometimes unreliable and incorrect.

Authors [37-40] have proposed novel method allowing reconstructing the LS energy distribution immediately from the SCLC CVC without the pre-defined model (the reverse task), for example, for organic materials with energetically wide LS distributions [41-42]. However, the expressions presented in [37-40], as shown by our studies [43-45], are not suitable for analysis of experimental data for mono- and polycrystalline samples with energetically narrow trap distributions. So, we use the principle [37-40] and obtain reliable and practically applicable expressions for working-out of the real experiments performed for traditional II-VI compounds.

Solving the Poisson equation and the continuity equation produces SCLC CVC for rectangular semiconductor samples with traps and deposited metallic contacts, where the source contact (cathode) provides charge carriers' injection in the material [24-25]:

$$j = e\mu E(x) n_f(x), \tag{1}$$

$$\frac{dE(x)}{dx} = \frac{e\left[\left(n_f(x) - n_{f0} \right) + \sum_j \left(n_{t_j}(x) - n_{t_{j0}} \right) \right]}{\varepsilon \varepsilon_0} = \frac{e n_s(x)}{\varepsilon \varepsilon_0}, \tag{2}$$

where *j* current density passes through the sample;

e electron charge;

μ drift carrier mobility;

ε₀ dielectric constant;

ε permittivity of the material

$E(x)$ is an external electric field changing by the depth of the sample; this field injects free carriers from the source contact (cathode) ($x=0$) to the anode collecting the carriers ($x=d$);

$n_f(x)$ is the free carriers' concentration at the injection;

n_{f0} is the equilibrium free carriers concentration;

$n_{t_j}(x)$ is the concentration of carriers confined by the traps of the *j*-group with the energy level E_{t_j} ;

n_{tj0} is the equilibrium carriers concentration trapped by the centers of the *j*-group;

$n_s(x)$ is a total concentration of the injected carriers.

The set of equations (1), (2) is commonly being solved with a boundary condition $E(0)=0$. The set is soluble if the function from n_f and n_t is known. We assume that all LS in the material are at thermodynamic equilibrium with corresponding free bands, then their filling-in by the free carriers is defined by the position of the Fermi quasi-level E_F. Using the Boltzmann statistics for free carriers and the Fermi – Dirac statistics for the localized carriers we can write [39-40]:

$$n_f(x) = N_{C(V)} \exp\left(\frac{E_{C(V)}(x) - E_F(x)}{kT} \right), \tag{3}$$

$$n_t(E,x) = \frac{h(E,x)}{1 + g \exp\dfrac{E_t(x) - E_F(x)}{kT}}, \tag{4}$$

where $N_{c(v)}$ are states density in conduction band (valence band);

$E_{c(v)}$ is energy of conduction band bottom (valence band top);

k is Boltzmann constant;

T is the temperature of measurements;

$E_F(x)$ is the Fermi quasi-level at injection;

g is a factor of the spin degeneration of the LS which depends on its charge state having the following values: $-1/2$, 1 or 2 (typically $g = 1$) [15, 39-40].

The zero reference of the trap energy level in the gap of the material will be defined relatively to the conduction band or valence band depending on the type (*n* or *p*) of the examined material: $E_{C(V)}=0$.

The set of equations (1)–(2) can also be reduced to integral relations. Detailed determination of these ratios presented in [37].

$$\frac{1}{j} = \frac{1}{e\mu d}\frac{\varepsilon\varepsilon_0}{e}\int_{n_{fc}}^{n_{fa}}\frac{dn_f}{n_f^2[(n_f - n_{f_0}) + \sum_j(n_{t_j} - n_{t_{j_0}})]} \equiv y,\tag{5}$$

$$\frac{U}{j^2} = \frac{\varepsilon\varepsilon_0}{e(e\mu)^2}\int_{n_{fc}}^{n_{fd}}\frac{dn_f}{n_f^3[(n_f - n_{f_0}) + \sum_j(n_{t_j} - n_{t_{j_0}})]} \equiv z,\tag{6}$$

where j, U are current density and voltage applied to the sample;
d is the sample thickness;
n_{fc}, n_{fa} are free carriers' concentration in cathode and anode, respectively.

Equations (5) and (6) determine SCLC CVCs in parametric form for an arbitrary distribution of LS in the gap of the material.

At thermodynamic equilibrium the total concentration (n_{s_0}), the carriers concentration for those localized on the traps (n_{t_0}), and the free carriers' concentration in the semiconductor (n_{f_0}) are in the function written as follows: $n_{s_0} = n_{t_0} + n_{f_0}$, де $n_{f_0} = N_{C(V)}\exp\left(-\frac{E_{C(V)} - E_{F_0}}{kT}\right)$ in case when $E_c - E_{F0} \geq 3kT$ ($3kT$= 0,078 eV at the room temperature; E_{F0} is the equilibrium Fermi level. It must be emphasized that this charge limits the current flow through the sample and determines the form of the SCLC CVC.

The carriers' injection from the source contact leads to appearance of the space charge ρ in the sample, formed by the free carriers and charge carriers localized in the traps, $\rho = en_i = e(n_s - n_{s_0}) = e[(n_t + n_f) - (n_{t_0} + n_{f_0})]$, where n_i is the concentration of injected carriers.

Under SCLC mode the concentration of injected carriers is considerably larger than their equilibrium concentration in the material and, at the same time, it is sufficiently lower than the total concentration of the trap centers ($n_{f_0} \ll n_i \ll N_t$) [24-25]. Thus, in further description we will neglect the second term in the expression written above (except some special cases). Then we have $\rho = en_s(x) \sim e\sum_j n_{t_j}(x)$.

Using (5) and (6) we find the first and second derivatives of z from y:

$$z' = \frac{dz}{dy} = \frac{d(U/j^2)}{d(1/j)} = \frac{d}{e\mu n_{fa}},\tag{7}$$

$$z'' = \frac{d^2 z}{dy^2} = \frac{d}{d(1/j)}\frac{d(U/j^2)}{d(1/j)} = \left|\frac{\rho_a d^2}{\varepsilon\varepsilon_0}\right|. \tag{8}$$

As the SCLC CVC are commonly represented in double-log scale [24-25], equations (7), (8) are rewritten with using derivatives: $\eta = \dfrac{d(\ln j)}{d(\ln U)}, \eta' = \dfrac{d^2(\ln j)}{d(\ln U)^2}, \eta'' = \dfrac{d^3(\ln j)}{d(\ln U)^3}.$

Then we have

$$n_{fa} = \frac{\eta}{2\eta - 1}\frac{jd}{e\mu U} = \frac{1}{\alpha}\frac{jd}{e\mu U}, \tag{9}$$

$$\frac{\rho_a}{e} = \frac{2\eta - 1}{\eta}\frac{\eta - 1}{\eta}\left[1 - \frac{\eta'}{\eta(2\eta - 1)(\eta - 1)}\right]\frac{\varepsilon\varepsilon_0 U}{ed^2} = \alpha\beta\frac{\varepsilon\varepsilon_0 U}{ed^2}, \tag{10}$$

where $\alpha = \dfrac{2\eta - 1}{\eta}$, $\beta = \dfrac{\eta - 1}{\eta}\left[1 - \dfrac{\eta'}{\eta(2\eta - 1)(\eta - 1)}\right] = \dfrac{\eta - 1}{\eta}(1 + B).$

Further we will neglect the index a.

As a result, the Poisson equation and the continuity equation give fundamental expressions for a dependence of the free carrier concentration in the sample n_f (the Fermi quasi-level energy) and space charge density at the anode ρ on the voltage U and the density of the current j flowing through the structure metal-semiconductor-metal (MSM).

Now let us consider the practical application of expressions (7) and (8) or (9) and (10) for reconstructing the trap distribution in the gap of the investigated material. We would restrict with the electron injection into n-semiconductor.

If the external voltage changes the carries are injected from the contact into semiconductor; at the same time, the Fermi quasi-level begins to move between the LS distributed in the gap from the start energy E_{F0} up to conduction band. This displacement ΔE_F leads to filling-in of the traps with the charge carriers and, consequently, to the change of the conductivity of the structure. Correspondingly, under intercepting the Fermi quasi-level and the monoenergetical LS the CVC demonstrates a peculiarity of the current [24-25]. As the voltage and current density are in the function of the LS concentration with in-advanced energy position and the Fermi quasi-level value we obtain a possibility to scan the energy distributions. This relationship is a physical base of the injection spectroscopy method (IS).

Increase of the charge carriers dn_s in the material at a low change of the Fermi level position is to be found from the expression:

$$\frac{1}{e}\frac{d\rho}{dE_F} = \frac{dn_i}{dE_F} \approx \frac{dn_s}{dE_F} \approx \frac{dn_t}{dE_F}. \tag{11}$$

The carrier concentration on deep states can be found from the Fermi-Dirac statistics

$$n_s = \int\limits_{E_1}^{E_2} n_s(E)dE = \int\limits_{E_1}^{E_2} h(E)f(E - E_F)dE + n_f, \tag{12}$$

where $dn_s(E)/dE$ is a function describing the energy distribution of trapped carriers;
$h(E)=dN_t/dE$ is a function standing for the energy trap distribution;
E_1, E_2 are energies of start and end points for the LS distribution in the gap of the material.

It is assumed that the space trap distribution in the semiconductor is homogeneous by the sample thickness then $h(E, x) = h(E)$.

After substitution of (12) in (11) we obtain a working expression for the functions $d\rho/dE_F$ and $h(E)$

$$\frac{1}{e}\frac{d\rho}{dE_F} \approx \frac{dn_s}{dE_F} = \frac{d}{dE_F}\int\limits_E n_s(E)dE = \int\limits_E h(E)\frac{d(f(E - E_F))}{d(E - E_F)} + \frac{n_f}{kT} \tag{13}$$

Thus, at arbitrary temperatures of the experiment the task of reconstructing LS distributions reduces to finding function $h(E)$ from the convolution (12) or (13) using known functions $n_s(E_F)$ or $d\rho/dE_F$. The expression (12) is the most preferable [39-40]. In general case the solution is complex and it means determining the function $h(E)$ from the convolution (12) or (13) if one of the functions n_s or dn_s/dE_F is known [43-45]. We have solved this task according the Tikhonov regularization method [46]. If the experiment is carried at low temperatures (liquid nitrogen) the problem is simplified while the Fermi-Dirac function in (13) may be replaced with the Heavyside function and, neglecting n_f, we obtain

$$\frac{1}{e}\frac{d\rho}{dE_F} \approx \frac{dN_t}{dE_F} \approx h(E). \tag{14}$$

This equation shows that the function $1/e \; d\rho/dE_F$ - E_F at low-temperature approximation immediately produces the trap distribution in the gap of the semiconductor. Using (7) and (8), we transform the expression (14) for practical working-out of the experimental SCLC CVC. As the free carrier concentration and the space charge density are to be written as follows:

$$n_f = \frac{d}{e\mu}\frac{j}{2U - U'j}, \tag{15}$$

$$\frac{\rho}{e} = (U''j^2 - 2U'j + 2U)\frac{\varepsilon\varepsilon_0}{ed^2}, \tag{16}$$

the expression (14) will be

$$h(E) \approx \frac{1}{e}\frac{d\rho}{dE_F} = \frac{1}{kT}\frac{\varepsilon\varepsilon_0}{ed^2}\frac{U'''j^3(2U - U'j)}{(U''j^2 - 2U'j + 2U)}. \tag{17}$$

Using derivatives η, η', η'' this expression is easily rewritten:

$$h(E) \approx \frac{1}{e}\frac{d\rho}{dE_F} = \frac{1}{kT}\frac{\varepsilon\varepsilon_0 U}{ed^2}\frac{2\eta-1}{\eta^2}\left[1+\frac{(3\eta-3)\eta\eta'-\eta\eta''+3\eta'^2}{\eta^2\left((2\eta-1)(\eta-1)-\eta'/2\right)}\right].$$ (18)

The expression (18) is also can be written with the first derivative (η) only. Denote

$$C = \frac{(3\eta-3)\eta\eta'-\eta\eta''+3\eta'^2}{\eta^2\left[(2\eta-1)(\eta-1)-\eta'/2\right]} = (2-3\eta)B+\frac{d\ln(1+B)}{d\ln U} = \frac{(2\eta-1)B+(3\eta-2)B^2+\dfrac{d\left[\ln(1+B)\right]}{d\ln U}}{1+(\eta-1)B},$$

where $B = -\dfrac{1}{\eta(2\eta-1)(\eta-1)}\dfrac{d\eta}{d\ln U}$.

We obtained an expression used by authors [39-40] for analysis of energetically wide LS distributions in organic semiconductors.

$$h(E) \approx \frac{1}{e}\frac{d\rho}{dE_F} = \frac{1}{kT}\frac{\varepsilon\varepsilon_0 U}{ed^2}\frac{2\eta-1}{\eta^2}(1+C) = \frac{\alpha\beta}{kT}\frac{\varepsilon\varepsilon_0 U}{ed^2}\frac{1}{\eta-1}\left(\frac{1+C}{1+B}\right).$$ (19)

To make these expressions suitable for the working-out of SCLC CVC for the semiconductors with energetically narrow trap distributions we write them with reverse derivatives $\gamma = \dfrac{d(\ln U)}{d(\ln j)}$, $\gamma' = \dfrac{d^2(\ln U)}{d(\ln j)^2}$, $\gamma'' = \dfrac{d^3(\ln U)}{d(\ln j)^3}$.

As a result:

$$h(E) \approx \frac{1}{e}\frac{d\rho}{dE_F} = \frac{1}{kT}\frac{\varepsilon\varepsilon_0 U}{ed^2}\left[\frac{(2\gamma-3)\gamma'+\gamma''}{(2-\gamma)(1-\gamma)+\gamma'}+\gamma\right](2-\gamma).$$ (20)

Solving the set of equations (3) and (7) gives energetical scale under re-building deep trap distributions. Using various derivatives we obtain

$$E_F = kT\ln\frac{e\mu N_{C(V)}}{d}+kT\ln\frac{2U-U'j}{j} = kT\ln\frac{e\mu N_{C(V)}}{d}+kT\ln\frac{j}{U}+kT\ln\frac{\eta}{2\eta-1} =$$

$$= kT\ln\frac{e\mu N_{C(V)}}{d}+kT\ln\frac{j}{U}+kT\ln\frac{1}{2-\gamma}.$$ (21)

Using sets of equations (17) - (18) or (20) - (21) allows to find a function describing the LS distribution in the gap immediately from the SCLC CVC. To re-build the narrow or monoenergetical trap distributions (typical for common semiconductors) the most suitable expressions are written with derivatives. The first derivative γ defines the slope of the CVC section in double-log scale relative to the current axis, the η defines the slope of the CVC section in double-log scale relative to the voltage axis. For narrow energy distributions this

angle η is too large, and under complete filling-in of the traps it closes to [24-25]. However, it means the slope to the current axis is very small allowing finding the first and higher order derivatives with proper accuracy [44, 45, 48]. It is important that the narrowest trap distributions give the higher accuracy under determination of the derivatives γ, γ', γ'' !

If the distributions in the semiconductor are energetically broadened all expressions (17), (18), and (20) can be used as analytically identical formulas.

As is seen from the expressions written above, in order to receive information about LS distribution three derivatives are to be found at each point of the current-voltage function in various coordinates. Due to experimental peculiarities we had to build the optimization curve as an approximation of the experimental data with it's further differentiation at the sites. The task was solved by constructing smoothing cubic spline [47]. However, the numerical differentiation has low mathematical validity (the error increases under calculation of higher order derivatives). To achieve maximum accuracy we have used the numerical modeling with solving of direct and reverse tasks.

Under solving the direct task we have calculated the functions ρ - E_F and $1/e\, d\rho/dE_F$ - E_F on base of known trap distribution in the gap of the material (the input distribution) using the expressions (12) and (13). Then we have built the theoretical SCLS CVCs ((5), (6)). The mathematical operations are mathematically valid. To solve the reverse problem of the experiment CVCs were worked out using the differential technique based on expressions (17), (21), (18), (20). As a result we have again obtained the deep centers' distribution in the gap of the material (output distribution). Coincidence of the input and output trap distributions was a criterion of the solution validity under solving the reverse task. Further the program set was used for numerical working-out of the experimental CVCs [43-45, 48].

2.2. Determination of deep trap parameters from the functions $1/e·d\rho/dE_F$ - E_F under various energy distributions

Now we determine how the energy position and the trap concentration under presence of the LS in the gap may be found for limit cases by the known dependence $1/e·d\rho/dE_F$ - E_F. In the case of mono-level the LS distribution can be written as $h(E) = N_t \delta(E - E_F)$, where δ is a delta-function.

After substituting this relationship in (12), (13) we obtain

$$n_s \approx n_t = \frac{N_t}{1 + g \exp\left(\dfrac{E_F - E_t}{kT}\right)}, \tag{22}$$

$$\frac{1}{e}\frac{d\rho}{dE_F} \approx \frac{dn_t}{dE_F} = \frac{g N_t \exp(\dfrac{E_F - E_t}{kT})}{kT(1 + g \exp(\dfrac{E_F - E_t}{kT}))^2}, \tag{23}$$

The value of the last function at the maximum ($E_F=E_t$) is $\left(\dfrac{1}{e} \dfrac{d\rho}{dE_F} \right)_{E_{Fm}} = \dfrac{gN_t}{kT(1+g)^2}$,

or at $g=1$ - $\left(\dfrac{1}{e} \dfrac{d\rho}{dE_F} \right)_{E_{Fm}} = \dfrac{N_t}{4kT}$..

Than

$$N_t = 4kT \left(\frac{1}{e} \frac{d\rho}{dE_F} \right)_{E_{Fm}}. \qquad (24)$$

Thus, building the function $1/e \cdot d\rho/dE_F$ - E_F and finding the maximums by using (24) gives the concentration of discrete monoenergetical levels. The energy position of the maximum immediately produces energy positions of these levels.

If the LS monotonically distributed by energy $h(E)=AN_t=$ const are in the gap of the material it is easy to obtain

$$N_t = h(E) = \frac{1}{e} \frac{d\rho}{dE_F}. \qquad (25)$$

In other words the trap concentration in the sample under such distributions is immediately found from the function $1/e \cdot d\rho/dE_F$ - E_F.

In general case when LS distribution in the gap of the material is described by the arbitrary function their concentration is defined by the area under the curve $1/e \cdot d\rho/dE_F$ - E_F and at low temperatures can be found from the relationship $N_t = \int_{E_1}^{E_2} h(E)dE$. Under reconstruction of such distributions from the SCLC CVC these distributions are energetically broadening depending on the temperature of experiment [43-45]. LS energy positions are again determined by the maximums of the curve.

The correct determination of the trap concentration from the dependence $1/e \cdot d\rho/dE_F$ - E_F may be checked out by using the function ρ - E_F. In case of the mono-level where the Fermi quasi-level coincides with the LS energy position, it is easy to obtain from (22) - $[n_t]_{E_{Fm}} = \dfrac{N_t}{1+g}$,

then $N_t = (1+g)[n_t]_{E_{Fm}}$. If $g=1$ then $[n_t]_{E_{Fm}} = N_t/2$, $N_t = [2n_t]_{E_{Fm}}$.

If the LS distribution is a Gaussian function ($h(E) = \dfrac{N_t}{\sigma_t (2\pi)^{1/2}} \exp\left(-\dfrac{E-E_t}{\sqrt{2}\sigma_t} \right)^2$) the relationship for determination of N_t is analogous to that described above.

Earlier [43-45] we have described the effect of experimental factors on accuracy of determining parameters of the deep centers by IC method. In Ref. [44, 45, 48] it was shown

that the neglecting third order derivative or even the second order derivative does not lead to considerable decrease of the accuracy in determination of the LS parameters. It was demonstrated that under neglecting the 3rd order derivative γ'' in (20) the error in definition of the function $h(E)$ at the point $E_F=E_t$ is no more than 0.4%. At the same time this error is somewhat larger in the interval $E_F-E_t{\sim}kT$ but is not larger than (4–7)%. Such a low error of the calculation of the LS parameters is caused by the interception of zero point and the derivative γ'' near the point $E_F=E_t$ (commonly in the range of $\left|E_F - E_t\right| < 0,2kT$). As a result (regarding the absence of accurate experimental measurement of the 3rd derivative) it does not affect the differential working-out of CVCs in the most important section where the Fermi quasi-level coincides with the LS energy position.

If the second order derivative in the working expressions is neglected the error of the defining the function $h(E)$ in the most principal ($E_F{\approx}E_t$) is about (30-40)%. In both cases the simplification of the expression (21) does not contribute errors to the definition of energy position of the traps' level. Remember that the traditional method of SCLC CVC gives 60-100% error of the traps' concentration [24-25].

3. Methods of preparation and investigation of II-VI films

Thin films CdTe, ZnS, ZnTe were prepared on glass substrates in vacuum by close-spaced vacuum sublimation (CSVS) [49-50]. For further electrical investigations we have deposited hard-melted metal conductive layers on the main substrate by electron beam evaporation (Mo – for CdTe, ZnS; Cr, Ti – for ZnTe). The up-source contact (In(Ag) or Cr in dependence on the conductivity type of the semiconductor) was deposited by the vacuum thermal evaporation. Under condensation of the films of binary compounds the chalcogenide stoichiometric powders were used.

The common temperature of the evaporator was T_e = 973 K for zinc telluride, T_e = (1200÷1450) K for zinc sulfide and T_e = (933÷1023) K for cadmium telluride. The substrate temperature was changed in a wide range T_s = (323÷973) K. Time of deposition was varied: t = (10÷30) min.

Morphology of the samples' surfaces was investigated by optical and electron microscopy. Jeffries' method was used to determine the arbitrary grain size (D) in the condensates. The films' thickness (d) was measured by fractography and interferential methods. The element composition of the layers was studied by X-ray spectroscopy (XRS) analysis using the energy-dispersed X-ray analysis (EDAX) unit or by Rutherford back scattering (RBS) technique (if it was possible). Structural examinations of the films were carried out by the XRD-unit in Ni-filtered K_α radiation of Cu-anode. The XRD patterns were registered in the range of Bragg angles from 20^0 to 80^0. Phase analysis was provided by comparison of inter-plane distances and arbitrary intensities from the samples and the etalon according to the ASTM data [51]. Structural properties of II-VI films are investigated in [20, 49-50, 54-56].

Dark CVC at different temperatures and $\sigma - T$ dependencies of the sandwich-structures (MSM were examined in vacuum by standard techniques (Fig. 1) [21-22].

The power of electronic scheme was estimated by source of stable voltage AIP 120/0.75 that provided a possibility of precise voltage regulation in electric circle in the ranfe of U =0.1 ÷ 120 V.

A current that passed throught samples in the range of I = (10^{-9}÷10^{-5}) A measured by digital nanoampermeter. Voltage drop on sample was fixed by digital multimeters APPA-108N and UT70B. Sample temperature at inveatigation of electro-physical properties controlled by authomatic feedback temperature controller "OVEN TRM10", input signal from it fed from chromel-alumel thermocouple.
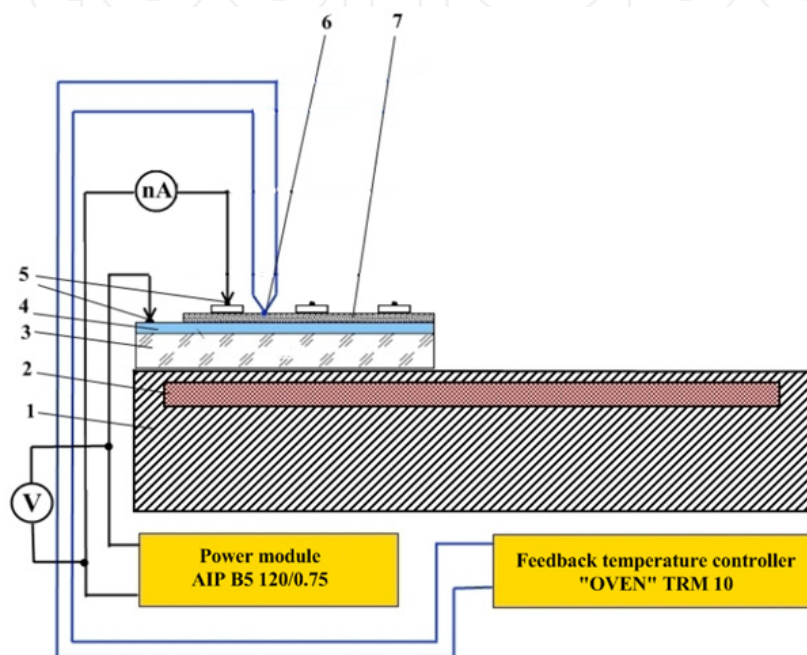

Figure 1. Typical electrical-type scheme for CVC and σ-T characteristic investigations of II-VI semiconductors films: 1 – heater holder; 2 – heater; 3 – glass substrate; 4 – lower conductive layer (Mo, Cr, Ti); 5 – collectors; 6 – thermocouple; 7 – II-VI film

The current mechanisms were identified by the differential method developed in [52-53]. This technique completely analyses j–U, γ–U and d(logγ)/d(log$U$)-U functions, where γ=d(log$j$)/d(log$U$) and differentiates satellite and concurrent current mechanisms in the structures and defines the high-field mechanisms among all of them. When the CVCs of multilayered structures were determined by unipolar injection from the source contact the experimental curves were numerically studied by using low-temperature and high-temperature approximations of the IS method [43-45, 48].

PL spectra of CdTe, CdSe and ZnTe films were studied using the spectrometer SDL-1 under excitation of the samples by Ar-laser (λ=514 nm for CdTe and λ=488,8 nm for ZnTe). PL spectra from ZnS films are registered by MPF-4 Hitachi and xenon bulb (λ=325 nm). The temperature in all experiments was stable in the range 4.7÷77 K by using the system "UTREX" [49]. The films CdTe, ZnTe were investigated in the range of edge luminescence, the films ZnS were studied in the impurity energy range.

At interpretation of the PL data it was suggested that the radiation had appeared as a result of electrons' transfer from the conduction (valence) band or shallow donor (acceptor) levels to the deep LS in the gap of the material. Then the activation energy of the processes are defined from the expression:

$$\Delta E = h\nu = E_g - E_i = E_g - (E_a + E_d),$$ (26)

where E_a, E_d are energy levels of the donors and acceptors in the gap of the material.

The set of methods for defining parameters of LS in the gap allowed to enhance the accuracy of data obtained and to examine traps and recombination centers with wide energy range.

4. Determination of LS parameters of polycrystalline chalcogenide films by injection spectroscopy method and analysis of $\sigma - T$ functions

4.1. General description of CVC and $\sigma - T$ functions

Dark CVC of sandwich structures current-conductive substrate-film-upper drain contact were measured at different temperatures for examining electrical properties of Zn and Cd chalcogenide films and determination of parameters for LS in the gap of material. Besides that, the function conductivity-temperature was studied in ohmic sections of the CVC and in some cases in the square section of the CVC. Energy positions of donor (acceptor) centers in the films were found from dependencies $\log\sigma = f(10^3/T)$ taking into account their Arrhenius-like character [21-22].

As was shown by the study, the CVC of multilayered structures MSM is defined by the condensation conditions of chalcogenide films, their crystal structure, and material of bottom and upper metallic contacts. CVC of multilayered structures based on low-temperature condensates of II-VI compounds were linear or sublinear. For ZnTe-based MSM structures the CVC were defined by the Pool-Frenkel mechanism, and the data were linearized in the coordinates $\log(I/U) - U^{1/2}$ [52].

Fig. 2 plots typical double-log CVC measured at different temperatures. This figure also shows the function $\sigma - T$ measured at the ohmic section of the CVC.

It is found out that the $\sigma - T$ function of low-temperature condensates are linear with the slope to the T axis decreasing at lowering the measurement temperature. These features are typical for the material with various types of donor (acceptor) impurities with different activation energy. The CVC of high-temperature condensates were somewhat others (Fig. 2). The linear sections are reveled, their slope to the T axis increases as the measurement temperature decreases. It is typical for compensated materials [21-22]. The compensation effect appears more visible under sufficiently low experimental temperatures when the electron concentration becomes close to that of acceptor centers. The slope of the straight lines to the T-axis increases from the value $E_a/2k$ up to the value E_a/k, making it possible to define activation energy for donor and acceptor centers [21-22].
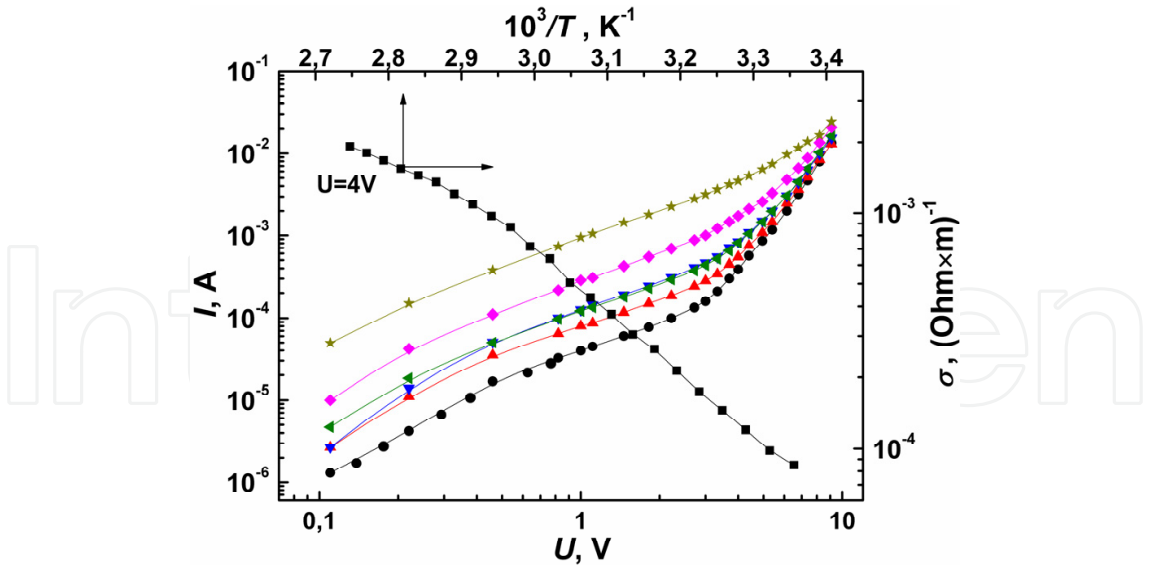
Figure 2. CVC of the structure Cr/ZnTe/Ag at various temperatures: • – T = 298 K; ▲ – T = 303 K; ▼ – T = 308 K; ▶ – T = 313 K; ♦ – T = 318 K; * – T = 323 K, and the dependence $\log\sigma$ – $1/T$ obtained from the ohmic section of the CVC. The film is prepared at T_e = 973 K and T_s = 823 K

CVC of multilayered structures where chalcogenide films are prepared at T_s > (500÷600) K were superlinear. As is analytically shown, they are determined by the unipolar injection from the drain contact. Typical SCLC CVCs of the examined films are plotted in Figs. 2-3. CVCs of high-temperature condensates in the range of high field strength a set of linear sections with various slopes to the U-axis was observed. As a rule, the sections with functions: $I – U$, $I – U^2$, $I – U^{3-5}$, $I – U^{8-10}$ were the most pronounced. In some cases after superlinear sections we have observed a square dependence I on U, which had further changed again to the supelinear one with a very large slope η ($\eta \sim 13–25$). The current jump was revealed and the samples were turn on the low-ohmic state as an irreversible process.
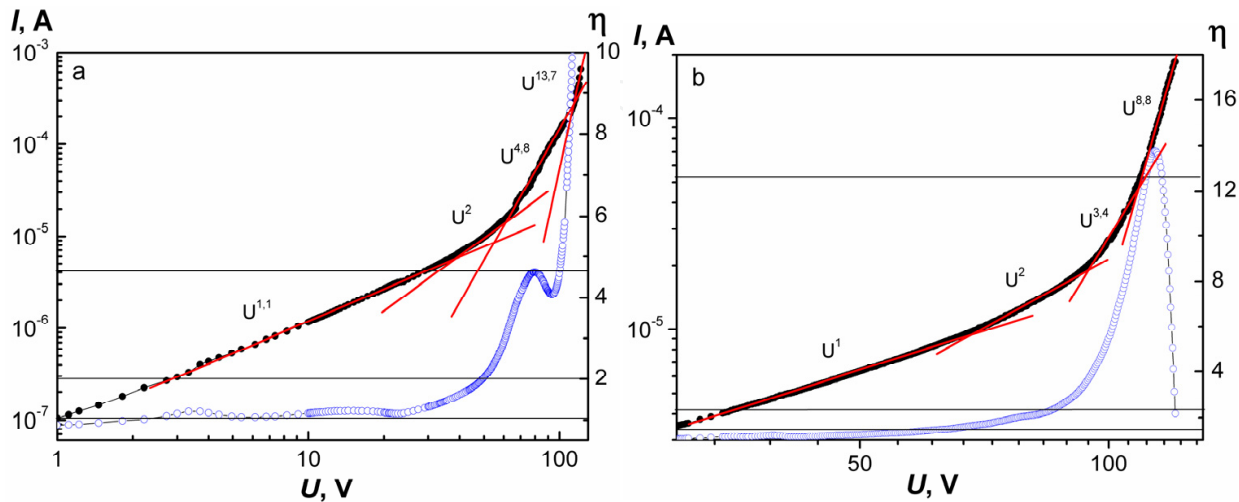

Figure 3. Double-log SCLC CVC of multilayered structures Mo/CdTe/Ag and results of their differentiation. CdTe films are prepared at T_e = 893 K and various T_s: 723 K (a); 823 K (b)

The features of the CVCs are clearly shown in functions $\eta - \log U$ giving a possibility to reveal a fine structure of the CVCs (Fig.3). Each point of this graph defines the slope of the CVC in double-log scale to the voltage axis. Dependencies $\eta - \log U$ were obtained by differentiating the CVC in every experimental point. As it was mentioned above, the problem mathematically reduces to the building smoothing cubic spline which approximates experimental data and its differentiation at the sites.

The curves $\eta - \log U$ resulting from the working-out of the SCLC CVC showed 1-4 maximums in correspondence to the sections of sharp current increase in the $I - U$ dependencies. The most often values of η_{ext} were 8–10. Sometimes the functions $\eta - \log U$ were practically revealed.

Horizontal sections with the almost constant slope $\eta > 2$ were also observed. It may be explained by the presence in the samples of sets of monoenergetical or quasi-monoenergetical levels traps of various energy position and concentration or by availability of the exponential (or other form) LS energy distribution. The specific points of CVCs were used for calculating trap parameters in the material, the ohmic sections helped to find specific conductivity of the layers $\sigma = (10^4 \div 10^5)$ $\Omega \cdot m$. As a result we obtained the concentrational distributions of the traps in the gap of material $h(E)$-E, their energy position (E_t) and concentration (N_t).

At the high voltage the CVCs are typical for the unipolar injection, but, according to [52-53] there some other current mechanisms leading to qualitatively similar current-voltage functions. Thus, we had to identify them additionally according to the procedure described in [52] by analyzing functions $\log I - \log U$, $\eta - \log U$ and $\log \eta - \log U$. It allowed identifying high-voltage current mechanisms in the samples and defining (in some cases) their type.

For further definition of the dominant current mechanism in the base chalcogenide layer we calculated the discrimination coefficient Q_{ext} in the extremum points of the function $\eta - \log U$ and compared it with coefficients typical for other mecahisms [52]. We have found $Q_{ext} > 10^6 \div 10^7$ almost in all cases, what is significantly larger than the values of Q_{ext} typical for the field trap ionization and the barrier –involved current mechanism in the material. This, in turn, points out [52-53] that the extremums in functions $\eta - \log U$ are caused by filling-in of the traps in the material with charge carriers injected from the metallic contact. Using various analytical methods allows to conclude with a good reliability that the CVC's features for multilayered structures with high-temperature chalcogenide layers ($T_s > 500$ K), were caused namely by the SCLC mechanism. Further we have worked out the CVCs due to injection currents only.

Fig. 4. illustrates a typical example of the CVC working-out. It is easy to see that the LS distributions are obtained under analysis of two different CVCs and they are in a good correlation.

To make the distribution more precise we have plotted in the same picture the Gaussian curve. It is seen that for examined polycrystalline CdTe films there are trap distributions in the gap with a form closed to that of the Gaussian one with a small half width σ_t.

Broadening energy levels in CdTe layers prepared by the vacuum condensation may be due to statistical dispersion of polar charge carriers' energy caused by fluctuative irregularities of the film crystalline lattice. This effect is enhanced near the substrate where the most defective layer of the film is grown. This region was an object for determining LS parameters by the method of SCLC CVC.
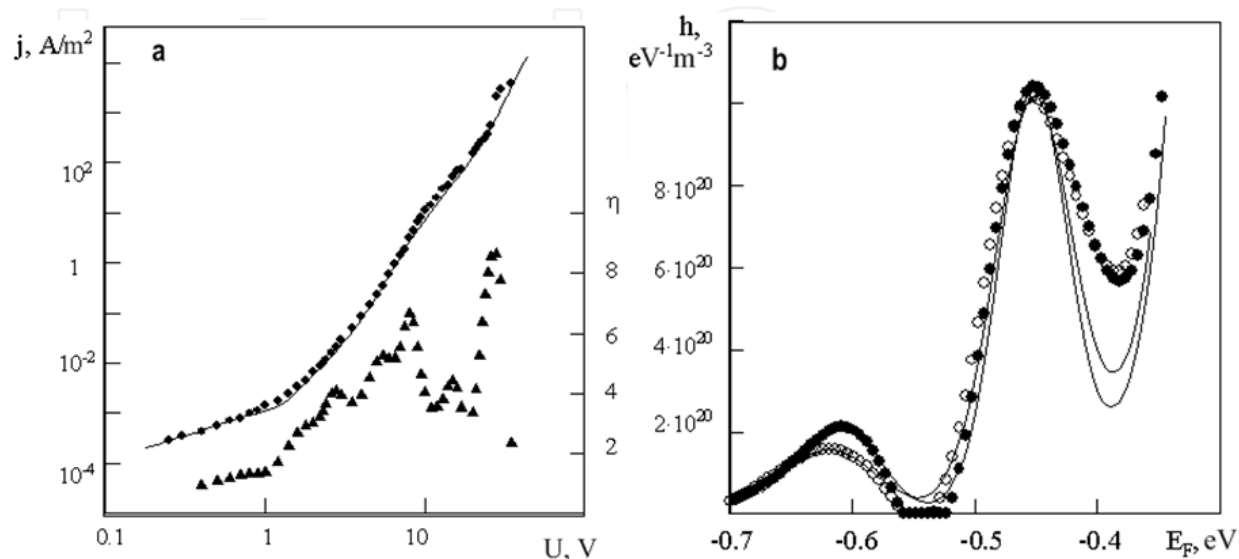

Figure 4. SCLC CVC and its derivative $\eta(U)$ for CdTe-based sandwich structures (a), and trap distribution in the gap of cadmium telluride (b): $\bullet$ – $j(U)$; $\blacktriangle$ – $\eta(U)$ (a); the energy trap distribution is resulted from the high-temperature IS method (b) ($\bullet$ – first measurement; o - repeating measurement at somewhat other temperature); the Gaussian distributions (solid line) are presented for comparison.

4.2. LS parameters from CVC and $\sigma - T$ functions

SCLC CVC was used for determination of trap parameters in the films. The low level of scanning LS spectrum was defined by the position of the equilibrium Fermi level E_{F0}, i.e. its position without charge carrier injection in the sample (ohmic section of the CVC), the upper limit was defined by the position of the Fermi quasi-level at the turn-on of the multilayered structures into low-ohmic state. The start position of the Fermi level was pre-defined by the equilibrium carrier concentration in the material, respectively, by the conductivity of the films. The calculations showed the position of the equilibrium Fermi level E_{F0} was coincide or was close to the energy of the deepest LS in the corresponding samples. The Fermi level is fixed by the traps because the concentration of free carriers in the films is close to the full concentration of LS located at grain boundaries and in bulk crystallites of condensates. As a result, the deepest trap levels located lower than the energy of the equilibrium Fermi level were not revealed in chalcogenide films by the SCLC CVC method.

The possibility of revealing shallow traps in the samples ($E_t \le 0.21$ eV, for ZnTe films) is restricted by their turn-on into the low-ohmic state stimulated namely by the LS. Thus, the SCLC CVC method had revealed the traps with energy higher positions. However, the traps with different energies also may exist in the samples as shown by the data from the slope of

conductivity-temperature functions in ohmic and square sections of the CVCs and luminescence spectra.

4.2.1. CdTe films

Table 1 presents some results of IS calculations for deep centers in polycrystalline and monocrystalline CdTe films. In the gap of the polycrystalline material are LS with E_1 = (0.68÷0.70) eV; E_2 = (0.60÷0.63) eV; E_3 = (0.56÷0.57) eV; E_4 = (0.51÷0.53) eV; E_5 = (0.45÷0.46) eV; E_6 = (0.39÷0.41) eV and concentration N = (10^{18}÷10^{20}) m^{-3}. The concentration of these LS is in the range N_t = (10^{18} ÷10^{21}) m^{-3} and mostly increases with closing their energy positions to the bottom of the conduction band. The traps by the profile $h(E) = N/\sqrt{2\pi}\sigma_t \exp\left(\Delta E^2/2\sigma_t^2\right)$ are similar to the mono-energetical ones with a half width $\sigma_t = (0.011\div0.015)$ eV. The dominant LS affecting SCLC CVC are the LS with energies E_t = (0.60÷0.63) eV; E_t = (0.56÷0.57) eV; E_t = (0.45÷0.46) eV. Only the traps (if revealed) with E_t = 0.40 eV had the larger concentration.

The LS were registered not only in polycrystalline films but also in monocrystalline layers. We have resolved the traps with E_t = (0.56÷0.57) eV; E_t = (0.52÷0.53) eV; E_t = (0.45÷0.46) eV and E_t = (0.40÷0.41) eV in the gap of the material. The monocrystalline condensates had lower resistance that the polycrystalline layers (10÷100 times), the equilibrium Fermi level in these films was placed more closely to the conduction (valence) band than that in polycrystalline films. Thus, the deepest traps were not revealed by SCLC CVC method in monocrystalline layers. So, the traps E_t ~ 0.70 eV and E_t ~ 0.62 eV found in polycrystalline films may be presented in lower-resistive monocrystalline films.

Ionization energies of the defects in the gap of CdTe were determined from the slope of functions conductivity-temperature in coordinate's $\log\sigma$-1/T [21-22]. Table 2 lists the results for polycrystalline and monocrystalline CdTe films. In high-temperature polycrystalline condensates the following activation energies were observed for conductivity: E_t=0.15; 0.33; 0.40÷0.41; 0.46; 0.60÷0.61, 0.80 eV. In the monocrystalline films the LS had smaller activation energy: E_t=0.06÷0.07; 0.13÷0.14; 0.22÷0.23; 0.29; 0.40; 0.46 eV. Activation energy E_t = (1.50÷1.52) eV is typical for high temperatures of the experiment and corresponds to the gap of the material. The comparison of the LS energy levels from the SCLC CVC and $\sigma - T$ functions is carried out in Table 2. The values E_t from the $\sigma - T$ functions correlate with those observed in CdTe films by SCLC CVC method.

The wide range of the traps revealed in CdTe condensates is obviously caused by investigation of disordered transition layer of the films formed under the film condensation near the substrate. In this layer may be presented foreign impurities adsorbed from the substrate and residual atmosphere under film condensation. Besides that for CdTe the concentration of uncontrolled residual impurities in the charge mixture can be N_t =(10^{20}-10^{21}) m^{-3} which is behind the sensitivity of the IS method. These impurities can form a chain of complexes impurity-native defect producing deep levels in the gap of the semiconductor.

Sample number	d, μm	T_s, K	T_e, K	E_t, eV	N_t, m^{-3}	σ_t, eV
1	8	743	1023	0.63	4.4·10^{19}	0.030
2 (1st measurement)	19	748	948	0.61	1.7·10^{19}	0.031
				0.45	7.3·10^{19}	0.028
2 (2nd measurement)	19	748	948	0.62	1.5·10^{19}	0.035
				0.45	8.1·10^{19}	0.032
3	12	748	968	0.68	7.8·10^{18}	0.023
				0.62	1.5·10^{19}	0.023
				0.53	6.1·10^{19}	0.027
4	9	723	893	0.62	6.6·10^{18}	0.021
				0.56	4.4·10^{19}	0.016
5	12	823	893	0.62	2.0·10^{18}	0.023
				0.57	1.7·10^{19}	0.015
6 (monocrystalline)	11	753	933	0.62	4.6·10^{18}	0.019
				0.52	1.3·10^{19}	0.009
				0.41	1.1·10^{20}	0.016
7	15	753	953	0.60	2.3·10^{18}	0.019
				0.52	3.6·10^{18}	0.020
				0.46	8.6·10^{18}	0.020
				0.41	1.4·10^{19}	0.015
8	26	758	978	0.61	3.6·10^{18}	0.023
				0.56	3.0·10^{19}	0.015
				0.52	7.4·10^{19}	0.015

Table 1. Parameters of LS revealed in CdTe films by high-temperature IS

E_t, eV			Interpretation
From SCLC CVC	From σ-T dependencies		
Polycrystalline films	Polycrystalline films	Monocrystalline films	
0.68-0.70	0.80	-	V_{Te}^{2+} (0.71 eV [57-61])
0.60-0.63	0.60	-	Te_{Cd}^{2+} (0.59 eV) [57-61]
0.56-0.57	0.57	-	Cd_i^{c2+} (0.56 eV) [57-61]
0.51-0.53	-	-	V_{Te}^{2+} (0.50 eV) [57-61]
0.45-0.46	0.46	0.46	Cd_i^{c+} (0.46 eV) [57-61]
0.39-0.40	0.40÷0.41	0.40	$Te_{Cd}^{2+} \cdot V_{Te}^{+}$ (0.40 eV) [57-61]
-	-	0.29	
-	-	0.22÷0.23	Cd_i^{2+} (0.20 eV) [57-61]
-	0.15	0.13÷0.14	
-	-	0.06÷0.07	

Table 2. Energetical positions of LS levels for defects in the gap of CdTe

As the chalcogenide films were not doped in-advance all LS found here are corresponding to native defects and their complexes with uncontrolled impurities. The interpretation is a challenge while the energy spectrum of PD in the gap of tellurium is studied not enough and identification in the most cases is not satisfactory (Table 3). For example, in [62] the levels E_t of LS are studied by photoinduced currents (PICTS) and authors give more than 150 values of deep levels, where the sufficient part of them is caused by the native defects. More reliables are some theoretical works where energies E_t are calculated («*ab anitio*») [57-61]. We have used namely the data Wei [57-58] obtained from the first principles. Table 3 summarizes our results.

According to calculations the deep centers with energy position 0.71 eV are belonging to V_{Te}^{2+}. We have experimentally observed the level $E_t = (0.68 \div 0.70)$ eV which may be caused by this defect. Analogically, the LS with energies $(0.60 \div 0.63)$ eV may be ascribed to the antistructural defect Te_{Cd}^{2+} (0.59 eV), and $(0.56 \div 0.57)$ eV and $(0.45 \div 0.46)$ eV to the interstitial cadmium in different charge states: Cd_i^{c2+} (0.56 eV), Cd_i^{c+} (0.46 eV). The level 0.29 eV is also formed by the native defect bound with cadmium Cd_i^{a2+} (0.33 eV). Different ionization energies of interstitial cadmium are due to its place in octo- or tetrahedral position in the crystal lattice of the material.

4.2.2. ZnTe films

Table 4.3 summarizes the results of calculations for ZnTe condensates in dependence on physical technical growth conditions. SCLC CVC method reveals set of trap groups with the most probable energy position $E_{t1} = 0.21$ eV; $E_{t2} = (0.32 \div 0.34)$ eV, $E_{t3} = 0.57$ eV; $E_{t4} = (0.41 \div 0.42)$ eV; $E_{t5} = 0.89$ eV. The concentration of the revealed LS is in interval $N_t = (10^{20} \div 10^{21})$ m^{-3}. The LS with energy $E_t = (0.32 \div 0.33)$ eV are dominant in the most samples and they determine the CVCs of the films.

The trap spectrum in ZnTe films can be partially checked by investigation of temperature – conductivity functions for the condensates. As shown by analysis of $\sigma - T$ functions in the Ohmic section of the CVC for high-temperature ZnTe condensates the following conductivity activation energies are typical: 0.05 eV; $(0.14 \div 0.15)$ eV; $(0.20 \div 0.21)$ eV; $(0.33 \div 0.34)$ eV; $(0.42 \div 0.43)$ eV; $(0.51 \div 0.52)$ eV; $(0.57 \div 0.58)$ eV; $(0.69 \div 0.70)$ eV and 0.89 eV (Table 4). Set of E_t values from the $\sigma - T$ functions is in a good correlation with those in ZnTe films defined by SCLC CVC method (Table. 3) and low-temperature luminescence (Table. 2).

As the films ZnTe as CdTe layers were not doped in-advance all the calculated LS are due to native PD, their complexes, uncontrolled impurities and their complexes with native defects.

The LS in monocrystals and films ZnTe were studied by SCLC CVC in [24, 63, 64]. Authors [24] have found the trap parameters in monocrystalline samples by the voltage of complete trap filling-in: $E_t = 0.17$ eV and $N_t = 10^{22}$ m^{-3}. On the other hand, measurements of $\sigma - T$ dependencies in the square section of the CVC gave $E_t = 0.14$ eV and $N_t = 10^{23}$ m^{-3} taking in mind the presence of traps in the material authors [64] calculated the LS density in ZnTe

films prepared by laser evaporation technique: $N_t = (4.2 \div 8.4) \cdot 10^{22}$ m^{-3}. The trap energy is not defined in this work. In ZnTe films obtained by the electro-deposition the trap concentration is $N_t = 3.6 \cdot 10^{21}$ m^{-3} [63].

Parameters of film condensation	From SCLC CVC		From σ-T dependencies	
	E_t, eV	N_t, m^{-3}	E_t, eV	N_t, m^{-3}
$T_s = 623$ K, $T_e = 973$ K	-	-	0.21	$2.1 \cdot 10^{20}$
	0.34	$8.6 \cdot 10^{20}$	0.34	$7.3 \cdot 10^{20}$
$T_s = 673$ K, $T_e = 973$ K	0.33	$5.3 \cdot 10^{20}$	-	-
$T_s = 723$ K, $T_e = 973$ K	0.34	$2.9 \cdot 10^{20}$	0.33	$4.1 \cdot 10^{20}$
	-	-	0.57	$5.5 \cdot 10^{20}$
	-	-	0.89	$8.4 \cdot 10^{20}$
$T_s = 773$ K, $T_e = 973$ K	0.32	$5.3 \cdot 10^{20}$	-	-
$T_s = 823$ K, $T_e = 973$ K	0.42	$2.1 \cdot 10^{20}$	-	-
$T_s = 873$ K $T_e = 973$ K	0.32	$1.5 \cdot 10^{21}$	-	-
$T_s = 623$ K $T_e = 973$ K	0.35 0.37	$8.8 \cdot 10^{20}$	-	

Table 3. LS parameters in ZnTe films from SCLC CVC and σ-T functions

As is seen from the Table 3, the trap concentration in ZnTe films is significantly lesser than that in condensates prepared by laser evaporation, electro-deposition methods and even in the monocrystalline material [23, 63- 64]. It shows a high structural perfectness and stoichiometry of the layers.

Nevertheless, the most levels found in ZnTe films may be identified with some probability. The level $E_1 = 0.05$ eV is commonly bound with single-charged dislocation V_{Zn}^{-}, and the level $E_2 = 0.15$ eV is bound with a double-charged V_{Zn}^{2-} Zn vacancy [65, 66]. In later works the second level is ascribed to Cu as to a traditional residual impurity in ZnTe, and the double-charged Zn vacancy is supposed to have a more deeper energy level 0.21 eV [66]. It is thought that the energy activation $(0.36 \div 0.40)$ eV [67, 68] is for the common substitution impurity in ZnTe, namely O_{Te}. The most deepest level 0.58 eV authors [67] ascribe to the Te vacancy V_{Te}^{2+} (interstitial zinc Zn_i^{2+}). The possible interpretation of LS in ZnTe films is listed in table 5.7. Other energy levels on our opinion are belonging to the uncontrolled impurities and complexes native defect-impurity.

We have revealed trap levels with energy position $E_t = (0.22 - 0.25)$ eV and concentration $N_t = (5.0 \cdot 10^{20} \div 1.5 \cdot 10^{21})$ m^{-3} by the analysis of SCLC CVC in ZnS films. These LS may be localized in the gap due to presence of the interstitial Zn atom Zn_i^{2+}. LS with energy position $E_t = (0.24 \div 0.25)$ eV were observed in [70] the thermo stimulated current technique.

T_s, K Section E_t, eV	623 Ohm.	623 Sq.	673 Ohm.	723 Ohm.	723 Sq.	773 Ohm.	823 Ohm	873 Ohm	Interpretation
E_9					0.89				–
E_8	0.70							0.69	–
E_7			0.58	0.58	0.57		0.58		$V_{Te}^{2+}(Zn_i^{2+})$ [67]
E_6	0.51		0.52			0.51	0.52		V_{Zn}^{2-} (0.50) [69]
E_5	0.43		0.42				0.42		O_{Te} (0.41) [67]
E_4	0.33	0.34	0.33		0.33		0.34	0.33	O_{Te} (0.36) [68]
E_3		0.21	0.20			0.20			V_{Zn}^{2-} (0.21) [67]
E_2						0.14		0.15	V_{Zn}^{2-}, Cu_{Zn}^{+} (0.15) [69]
E_1		0.05							V_{Zn}^{-} (0.05) [65]

Table 4. Energy positions of LS for defects in ZnTe gap determined from the slope of σ–$1/T$ functions

According to the Arrhenius equation σ-T functions allowed calculating conductivity activation energies in linear sections: E_1=0.03 eV; $E_2 = (0.07 \div 0.08)$ eV, $E_3 = 0.15$ eV; $E_4 = (0.23 \div 0.24)$ eV; $E_5 = 0.33$ eV; $E_6 = 0.46$ eV; $E_7 = 0.87$ eV.

4.2.3. ZnS films

Table 5 summarizes LS parameters calculated by SCLC CVC method and from the σ-T functions in ZnS condensates prepared under various physical technical conditions. Reference data are presented for comparison. The table shows a correlation between our results and data obtained by other authors [71-74]. Besides that, there is a coincidence of defect energy positions defined from the SCLC CVC and σ-T functions.

T_s, K ($T_e = 1173$ K)	From CVC SCLC E_t, eV	From CVC SCLC N_t, m⁻³	From σ-T dependencies E_t, eV	From σ-T dependencies Reference data
523 K	0.22	$5{,}1 \cdot 10^{20}$	0.03	0.029 [71]
			0.07	0.06 [72]
590 K	0.25	$1.5 \cdot 10^{21}$	0.07	0.06 [72]
			0.24	0.24; 0.25 [70, 72]
			0.33	0.31-0.33 [70]
			0.87	0.81-1.29 [74]
673 K	0.23	$8{,}2 \cdot 10^{20}$	0.03	0.029 [71]
			0.23	0.24; 0.25 [70, 72]
			0.15	0.14 [72, 73]
			0.46	-

Table 5. LS parameters defined by analysis of SCLC CVC and σ-T functions at ohmic section of the CVC for ZnS films prepared under various physical technical condensation modes

All the LS found here were not identified because of absence of corresponding reference data. Only the levels with activation energy $E_1 = 0.15$ eV and $E_2 = (0.22 \div 0.25)$ eV may be bound with single- Zn_i^+ and double charged Zn_i^{2+} interstitial Zn atom.

5. Determination of LS parameters of polycrystalline chalcogenide films by optical spectroscopy (low-temperature photoluminescence)

Low-temperature photoluminescence (PL) is one of the most reliable tools applied for investigation of longitudinal, native, impurity and point defect ensembles in semiconductors. High resolution of the method makes it possible to examine not only bulk materials (bulk chalcogenide semiconductor are now good studied [75-87, 90-93, 96, 99-100, 102-104]), but also thin films, in particular, chalcogenide semiconductor thin layers. In this part we present data obtained by studying low-temperature PL spectra of ZnTe, CdTe and ZnS films. These results allowed monitoring and adding new results to those given by the IS method.

5.1. CdTe films

Fig. 5 (a, b) illustrates the typical spectra of these films. As shown, the spectra for both types of the films are significantly similar. A modest energetical displacement of lines in spectra from epitaxial films comparing to those from the polycrystalline layers films deposited on glass may be caused by presence of sufficient macrodeformations in the layers CdTe/BaF2. PL spectra from CdTe layers have lines originated from optical transfers with participation of free and bound excitons, transfers valence band – acceptor (e-A), donor-acceptor transfers (DAP), the radiation caused by presence of dislocations or DP (donor pairs, DP) (Y - stripes); the spectra also have a set of lines corresponding to optical transitions where phonons take place (LO - phonon replica) [87-99].
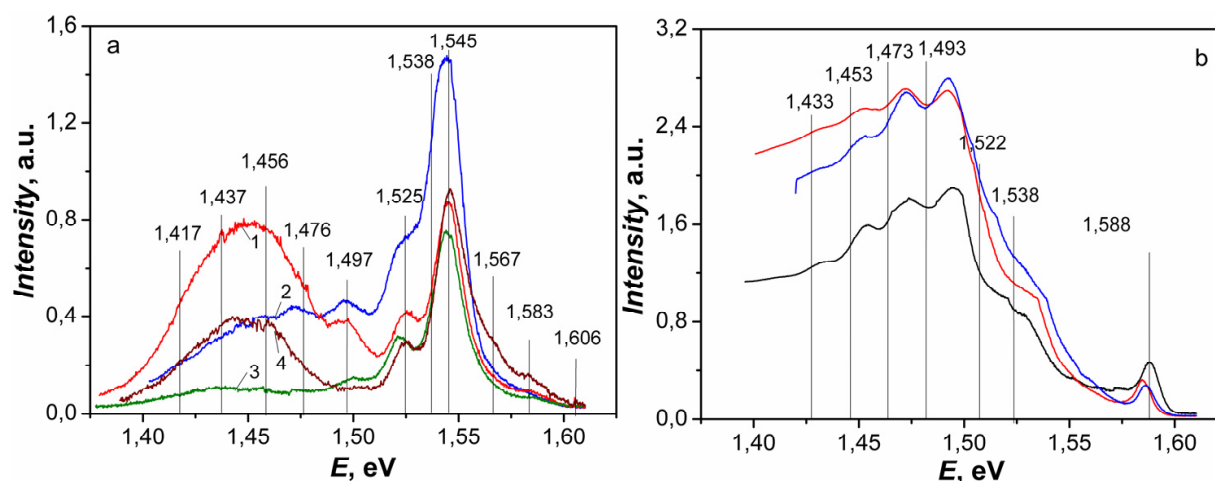

Figure 5. PL spectra registered at T=4,5 K for polycrystalline films CdTe/glass (a), prepared at $T_e = 893$ K and various T_s, K: 473 K (1); 523 K (2); 623 K (3); 823 K (4) and for the epiraxial layer CdTe/BaF2 (b): $T_e = 893$ K, $T_s = 798$ K

Activation energies relative to the valence band (while the most samples were of p-type conductivity) were calculated using expression (26) (in analogy with description above).

The gap of CdTe at T=4.5 K was supposed to be E_g =1.606 eV. The data are presented in Table 6.

E_i, eV	Reference data, eV	ΔE_i, eV	Recombination type	Interpretation
1.583	1.589-1.588	0.023	Exciton	A^0X, A -Li, Na [90, 92, 95, 99, 100]
1.567	1.568	0.039	Exciton	(A^0X)-LO [90, 100]
1.545	1.546	0.061 (0.050) [13] (0.058-Li. Na)	e-A - - DAP	A- V_{Cd}^- [13, 94, 95] $A - Li$, Na [90, 92, 99] $(V_{Cd} - O_{Te})$-[97, 102] $D - V_{Cd}^-$ [13, 103]
1.538	1.538	0.068 (0.067-V_{Cd})	DAP -	$D - A$ [93] $D - A$ (Na) [13, 92]
1.525		0.081	(e-A) LO	[97]
1.497	1.496 1.499 1.495	0.109 (0.107 [13]) (0.111 [13])	e-A - -	O [99] Ag_{Cd} [13] V_{Cd}^{2-} [13]
1.476	1.474 1.477	0.130	e-A	Y [96-99, 101] Y (α-dislocations [93]
1.457	1.459	0.149 (0.146 [13, 92])	e-A - - DAP	$(A-X)$-LO [101] Y [91] Cu_{Cd} [13] $\left(In - V_{Cd}^{2-}\right)^-$ [13, 92, 100]
1.438	1.436	0.168	e-A DAP	$(A-X)$-$2LO$ [101] $\left(In - V_{Cd}^{2-}\right)^- - LO$ [13, 92, 100]
1.419	1.415	0.187	e-A DAP	$(A-X)$-$3LO$ [101] $\left(In - V_{Cd}^{2-}\right)^- - 2LO$ [13, 92, 100]

Table 6. Principal lines of PL spectra of CdTe films and their interpretation

The lines due to exciton recombination in CdTe single crystals are well-known. Authors [13] show energy level diagram for the exciton localized on neutral donors or acceptors and possible transfers between these levels. Commonly the elements of 3rd Group (Ga, In, Al) and 7th Group (Cl, Br, I) are shallow donors in CdTe and ZnTe, and acceptors are the elements of 1st Group and 5th Group (Li, Na, Cu, Ag, Au, N, P, As). These elements are typical excessive impurities in compounds II-VI. Authors [13] also give the ionization energies of principal dopant impurities in CdTe: for the donors (13.67÷14.48) meV, for

acceptors 56 (N) - 263 (Au) meV. We have used these values for further interpretation of the experimental results.

Unlike ZnTe condensates the peak bound with a free exciton recombination at energies E_i = 1.596 eV [12] had not been observed for CdTe films. However, the spectra showed a line caused by the recombination of exciton localized on neutral acceptor A^0X - E_i = (1.583÷1.588) eV (1.589 eV [90, 92, 95, 99, 100]). This line indirectly demonstrated that the investigated films were of p-type conductivity and correspondingly low concentration of dopant impurities. Maybe there is a reason for absence of the peak bound with the exciton localized on the neutral donor D^0X – 1.593 eV [13, 90, 100] in the registered spectra. The excessive impurity (Li, Na) commonly is an acceptor in II-VI compounds which produces shallow LS near the valence band.

In some PL spectra of CdTe films we have observed the peak due to the phonon repetition of the line from the bound exciton (A^0X)-LO at E_i = 1.567 eV. The similar peak with E_i=1.568 eV and E_i=1.570 eV was also observed in [90, 100]. It should be noted that the excitation energy of the longitudinal phonon in CdTe is LO(Γ) – 21.2 meV [13, 90, 92]. This value is almost coinciding with that observed experimentally (21 meV) showing our correct interpretation of the experimental data.

The most intensive peak of 1.545 eV was observed in PL spectra from polycrystalline films. The similar peak with energies E_i=1.55 eV and E_i=1.545 eV was registered by authors [92, 94, 97, 99, 103]. The common interpretation says that this peak is caused by the electron transition between the conduction band and acceptor (e-A) (a single-charged vacancy V_{Cd}^- [94] or other shallow acceptor [92, 99]). Nevertheless, authors [13, 95, 103] point out this radiation as a consequence of p resenting donor-acceptor pairs (DAP) where the acceptor is a native defect (V_{Cd}^-) [13, 103] or another uncontrolled shallow impurity [95]. Authors [97] have found the activation energy of corresponding donors and acceptors: 8 meV and 47meV.

Results of investigated polycrystalline CdTe films in hetero structures CdTe/ZnS under air and vacuum annealing have given [97] another interpretation. It is supposed that the luminescence with 1.55 eV is due to oxygen presence in the material. In which form it exists in the material (substitutional impurity or oxide phase) is not established. However, authors [102] have studied the LS in CdTe single crystals by thermo electronic spectroscopy and demonstrated the energy level 0.06 eV bound with a complex ($V_{Cd} - O_{Te}$)⁻.

Analyzing our results allows us to conclude that the peak E_i=1.545 eV is rather due to the electron transitions between the conduction band and acceptor (a single-charged vacancy or DAP). Really if this peak was caused by oxygen we could it observed in PL spectra from both polycrystalline and epitaxial films but there are no such a peak in PL spectra from the films CdTe/BaF2. Besides that no structural method had revealed the oxygen in these compounds The films under investigation have shown no registered donor impurities of considerable concentration, so the interpretation of this peak as a consequence of the DAP presence is lesser probable than that a consequence of e-A transition.

In some cases the PL spectra from the polycrystalline films showed an asymmetric peak 1.545 eV indicating that in reality it may be a superposition of two nearest lines. Mathematical analysis showed that the most probable position of the additional peak is E_i = 1.538 eV. The similar peak was observed in spectra from the epitaxial films CdTe/BaF$_2$. The line with the same energy was revealed by authors [93] in PL spectra from deformed CdTe single crystals and is supposed to be caused by defects generated in the material due to slip of principal Cd(g)-dislocations. Authors [13, 92] explain the peak E_i= 1.538 eV as one of unknown nature. Similar interpretation is also in [89] where the line E_i= 1.539 eV is caused by DAP (here the acceptor is sodium, Na_{Cd}). The next peak E_i = 1.525 eV is likely is the phonon repetition of the previous one (e-A)-LO [96].

The PL line E_i = 1.497 eV was observed in [99] on monocrystalline CdTe samples under doping by ion implantation. As this line has appeared in the samples doped with oxygen only the authors suggest it is caused by the presence of this impurity. Other authors suppose this line is due to electron transitions between the conduction band and the level of the substitutional impurity acceptor Ag_{Cd} (E_v+0.107 eV) [13] or by native defect V_{Cd}^{-2} (E_v+0.111 eV) [13].

The wide radiation stripe in polycrystalline films at the energy 1,45 eV is separated in single peaks based on results from the PL of epitaxial films. They are shown in Fig. 5.

The peak 1.476 eV in [96-98] is due to longitudinal defects (dislocations and DP, a so-called Y-stripe). Authors [90, 98] assume the Y-stripe at (1.46-1.48) eV is caused by longitudinal defects (dislocations). Authors [99] make it more precicely: this peak is caused by the recombination of exciton localized on slipped Cd-dislocations. Authors [93] have investigated The photoluminescence of deformed CdTe single crystals and showed that the peak E_i=1.476 eV is not caused by the Cd-dislocations but is due to the electron states of 60^0 Te(g)-dislocations (α-dislocations). So that, the number of authors have the same opinion that this line in PL spectra is caused by the longitudinal defects. We also agree with this interpretation.

The lines 1.453 eV, 1.433 eV and 1.413 eV which are good resolved in spectra from the epitaxial films CdTe/BaF$_2$ are very similar to 1LO, 2LO, 3LO repetitions of the peak E_i = (1.473÷1.476) eV. However, the energy difference of these lines (ΔE=0.0200 eV) does not coincide with the energy of longitudinal optical phonons in CdTe 0.0212 eV making it difficult to interpret the corresponding peaks unambiguously. At the same time, the analogous set of lines with the LO structure and the energy difference 0.0200 eV in the range ΔE = (1.39÷1.45) eV was observed by authors [101]. They have studied polycrystalline CdTe films deposited by vacuum evaporation at T_s= (723÷823) K on glass and aluminum substrates.

Authors [100] have examined undoped and doped with donor impurities (Al, In) CdTe single crystals and also have observed the PL stripe in the energy range ΔE = (1.380÷1.455) eV containing four lines with LO structure. The authors interpreted them as electron transition between DAP and their phonon repetitions. Authors [81, 91] suppose the wide peak 1.46 eV is due to the excitons localized in longitudinal defects, probably dislocations

(*Y*-stripe). The lines 1.455 eV, 1.435 eV and 1.415 eV were observed in [94] from the polycrystalline CdTe films prepared by the gas-transport method.

As we see the most authors have an unique opinion: the set of lines in the range ΔE=(1.413÷1.476) eV is due to longitudinal defects (rather dislocations), and their intensity [93] can be a measurement unit of these defects in the material.

For polycrystalline films (Fig. 5, a) the LO structure of the stripe caused by the longitudinal defects at energies ~1.45 eV has practically not been observed, maybe because of superposition with additional lines of another origin.

The defect complexes in the material (A-centers) are also resolved by the PL in the same energy range (it can be considered as a partial case of DAP). According to [13, 97] A- centers $\left(V_{Cd}^{2-} - D^+\right)^-$ where Cl is a donor produce the line and its LO-phonon repetitions with energies 1.454, 1.433, 1.412, 1.391, 1.370, 1.349 and 1.328 eV. However, as is seen in Fig. 5, this stripe is displaced relatively to that observed experimentally, so the experimental PL spectra of CdTe films can be completely explained by these complexes only. The narrower stripe with peaks 1.458, 1.437, 1.417 and 1.401 eV produces the A-center where indium is a donor. This stripe has the better coincidence with experimental one but is also displaced. Besides that, it is difficult to explain why the A-complex is observed in the polycrystalline films and is not observed in the epitaxial layers while the charge mixture for both types of the films is the same. Thus we suppose the interpretation of the wide stripe in the energy range $\Delta E = (1.413÷1.4760)$ eV due to longitudinal defects is more reliable.

Under change of condensation conditions of polycrystalline samples we have observed the change of intensity for a stripe due to prolonged defects (~1.45 eV). As shows Fig. 5, as the substrate temperature increases from 473 K to 623 K the intensity of this stripe is decreasing and then it increases as the T_s increases. These results have a good correlation with data of investigation of CdTe film substructure [49], this fact points out an enhance of the structural quality (lowering vacancy concentration) of the bulk crystallites in condensates under elevating substrate temperature up to T_s=623 K, but this quality becomes lower as the substrate temperature increases over 623 K.

As the substrate temperature elevated (T_s>723 K) the optical properties of CdTe films were strongly degraded forming a number of additional peaks in the PL spectra which finally become a bell-like curve without possibility to identify the separate lines. Morphological studies demonstrated further increase of the crystallite sizes in this temperature range. However, the volume of these crystallites becomes a high-defective one.

Table 6 summarizes results of PL spectra interpretation for CdTe films showing their high optical quality.

5.2. ZnTe films

Fig. 6 illustrates typical PL spectra of ZnTe films registered at 4.5 K. A number of lines is observed, their energies are indicated in the Fig. 6 and are listed in Table 7. Analysis and interpretation of the PL peaks are carried out according to reference data [75-89].

The low-temperature PL spectra of ZnTe films show a set of peaks originated from: i) optical transitions under participation of free (X) and bound on neutral donor (D^0X) and acceptor (A^0X) excitons; ii) transitions valence band – acceptor impurity (e-A), iii) radiation due to presence of longitudinal defects (dislocations, Y-stripe); iv) optical transitions where phonons of different type are participating (LO (0.0253 eV), TO, LA (0.0145 eV), TA (0.007 eV) -repetition).

We calculated activation energies of corresponding processes using the expression (26). The gap of ZnTe crystal at 4.5 K was supposed to be E_g = 2.394 eV. As the examined material was of p-type conductivity the activation energies were counted down relative to the valence band. Table 7 summarizes these data.
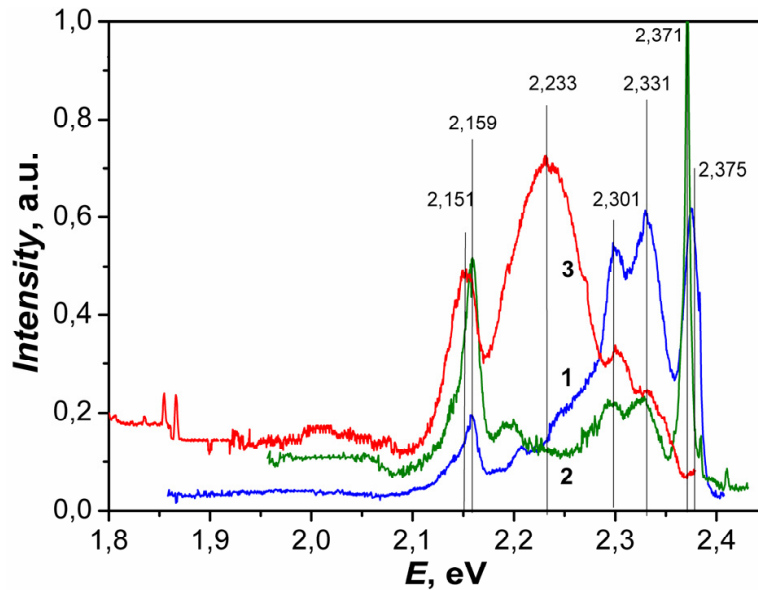

Figure 6. Photoluminescence spectra registered at T=4.5 K for ZnTe films prepared at T_e = 973 K and various T_s, K: 573 K (1); 673 K (2); 773 K (3)

Optical transitions with energy (2.381÷2.383) eV were observed in [68, 75-82, 84-86] where authors had studied monocrystalline or bulk polycrystalline ZnTe of high structural and optical quality. These transitions are commonly relating to a free exciton (X). Earlier [82] the PL line of E_i = (2.374÷2.375) eV was suggested to be caused by the exciton bound on neutral acceptor (zinc vacancy V_{Zn}). Further [76-78] it was shown that other acceptor centers take part in forming such an excitonic complex, in particular, acceptor centers due to uncontrollable impurities (Li, Cu) in ZnTe are of interest. However, in the most recent works [68, 81] this line is ascribed to the exciton localized on shallow neutral donor (atoms of uncontrollable impurities from 3rd and 7th Groups of the Periodical System (In, Ga, Al, Cl, Br. I)). These impurities form in the gap of the material more narrower levels than the acceptor ones. The line with E_i=2.371 eV which is energetically closed to that considered above is due to radiation of bound excitons [76-78, 81]; nevertheless the impurity (acceptor) in this complex has (obviously) somewhat larger energy level causing other energy of the stripe. These acceptors are native defects and uncontrollable excessive impurities (Li, Na, Ag, Cu).

According to [81] Li_{Zn} is the most probable candidate while it forms in the gap of the material energy level 60.6 meV.

Radiation line E_i, eV	Reference data, E_i, eV	Activation energy, ΔE, eV	Recombination type	Interpretation
2.383	2.381÷2.383	0.011	Exciton	X, n=1 [68, 76, 82]
2.375	2.375 2.379	0.019	Exciton	A^0X [76-77] A- V_{Zn} [82] D^0X, D- In [68, 86]
2.371	2.374; 2.375	0.023	Exciton	A^0X, A-Li,Cu [68]
2.331	2.334; 2.332	0.060 (0.061 – Li [75, 78]) (0.063 – Na [75])	e-A	A - Li_{Zn}, Na_{Zn} [75, 76]
2.301	2.307	0.093	(e-A)-LO	A - Li_{Zn} [76-77]
2.270	2.270	0.124	e-A	A - Ag_{Zn} [76]
2.233	2.230	0.161	e-A	A - Cu_{Zn} [75, 79]
2.208		0.186		
2.194	2.195; 2.19	0.200	e-A	Y_1 [75]
2.159		0.235		
2.151	2.155	0.243	e-A	Y_2 [75, 76, 78, 84]

Table 7. Principal lines in PL spectra of ZnTe films and their interpretation

It should be noted that the presence of excitonic lines in PL spectra from high-temperature ZnTe condensates points out their high optical and crystal quality. These lines are of sufficient intensity in the spectra from the films deposited at the substrate temperature T_s=573 K and the larger intensity for condensates prepared at T_s=673 K. Excitonic lines in the spectra from low-temperature condensates and layers manufactured at T_s>773 K were not registered. Thus, the results of PL studies indicate that the films deposited at the substrate temperatures T_s= (623÷673) K are the most optically perfect layers. These data are coinciding with the results of investigations of substructural characteristics of ZnTe films reported earlier [54]. According to these data the dependence of the CSD sizes on the substrate temperature is a curve with the maximum at T_s = (600÷650) K. The minimal dislocation concentration is also observed in the films under these temperatures.

The line E_i = 2.34 eV belonging [66] to V_{Zn} is not observed in spectra of the radiation recombination in ZnTe films. This fact is also confirming high stoichiometry of the films under study.

The set of nearest lines in the energy range ΔE = (2.30÷2.33) eV and ΔE = (2.17÷2.25) eV authors [76-79] ascribe to the electron transitions from the conductance band to the shallow acceptor levels formed by Li or Cu atoms and their phonon repetitions (LO – 25.5 meV). There are stripes $2S$Li, $3S_b$Li, (e-A) Li, 2P Li, $4S_b$Li, $4S_b$Li-LO, $2S$Cu, $3S_b$Cu, $4S_b$Cu, $2S_b$ Cu - LO, $2S_b$ Cu - 2LO and others. Experimental and theoretical values of the activation energy for ground and excited states for the main excessive impurities in ZnTe (lithium and copper)

are reported in [76]. They are in the energy range ΔE = (0.0009÷0.0606) eV for Li and ΔE = (0.001÷0.148) eV for Cu. However, in [65] the line E_i = 2.332 eV is supposed to be due to other excessive impurity Na_{Zn}, and in [82] this line is due to the native defect V_{Zn}. Another optical transition E_i = 2.27 eV authors [77] ascribe to the Ag impurity 2S Ag.

What about the peaks in the energy range E = (2.10÷2.21) eV. These transitions were for the first time observed in [75-79] and authors had called them Y_i-lines. They are ascribed to the distortions of the crystalline lattice of the material near incoherent twin boundaries, dislocations and other longitudinal defects where the dangling bonds are formed in the semiconductor material. So that, the lines E_i = 2.159 eV and E_i=2.194 eV can be interpreted as Y_2 (2.155 eV) and Y_1 (2.195 eV) [75]. They are due to longitudinal defects and the change of their intensity may point out the change of these defects concentration in the material. Somewhat other energy position of the line due to oxygen (2.06 eV) is reported in [66]. Thus, analysis of the reference data has forced us to conclude that PL lines in the energy interval ΔE = (1.835÷2.055) eV are rather caused by oxygen, its complexes and phonon repetitions. If it is true, the analysis of PL spectra from ZnTe films indicates the increase of the oxygen content in the samples under increasing the condensation temperature. Actually, if there is no oxygen in the samples prepared at 573 K, its concentration in high-temperature films (T_s=773 K) is sufficiently larger. Oxygen concentration in the material strongly depends on the vacuum conditions under the film preparation and the charge mixture quality.

5.3. ZnS films

Low-temperature photoluminescence is the most reliable tool for examining wide gap materials providing minimization of overlapping peaks due to various recombination processes. The typical PL spectra from ZnS films at 4.7 K are shown in Fig. 7. The detailed analysis of the PL spectra (identification of complex broadened lines) was carried out by ORIGIN program. Maximums of the peaks revealed by this analysis (Fig.7) are noted by vertical lines.

It should be noted that the PL spectra registered at various temperatures of experiment have no sufficient distinctions except those with somewhat larger line intensities in spectra obtained at 77 K. Analysis of the spectra shows that for ZnS films deposited at T_s = (393-613) K the peaks with λ_i = 396 nm (E_i = 3.13 eV) and λ_i = 478 nm (E_i=2.59 eV) are dominating. Further working-out of the spectra demonstrated that the peak λ_i= 396 nm is asymmetric (Fig. 7) what is may be explained by the superposition of two closely placed lines. The spectra also have low intensity peaks with λ_i =603 nm (E_i=2.06 eV) and λ_i =640 nm (E_i=1.94 eV).

PL spectra from the films prepared at higher T_s is sufficiently changed. There is a number of overlapping peaks where the most intensive ones are in the wavelength range $\Delta\lambda_i$ = (560÷620) nm.

Under interpretation of PL spectra from ZnS films we have calculated the activation energies of processes causing the corresponding lines. We also have suggested the PL

radiation took place under transfers of electrons from the conduction band (or shallow donors) to the deep LS in the gap of the material. Then the optic depth of the energy level of the defect (ΔE) relative to the valence band causing the spectral peak may be found from (26) supposing the optical gap of the material at 4.5 K is $E_g = 3.68$ eV.

Taking into account that the chalcogenide films were not doped in-advance one can suggest that the lines in spectra are due to transfers of carriers between conduction band and LS caused by the native point defects, their complexes and uncontrolled impurities. We made an attempt to identify these LS according to reference data [104-108] (Table 8). As is shown there is a good correlation of our results and those obtained by other authors for ZnS single crystals.
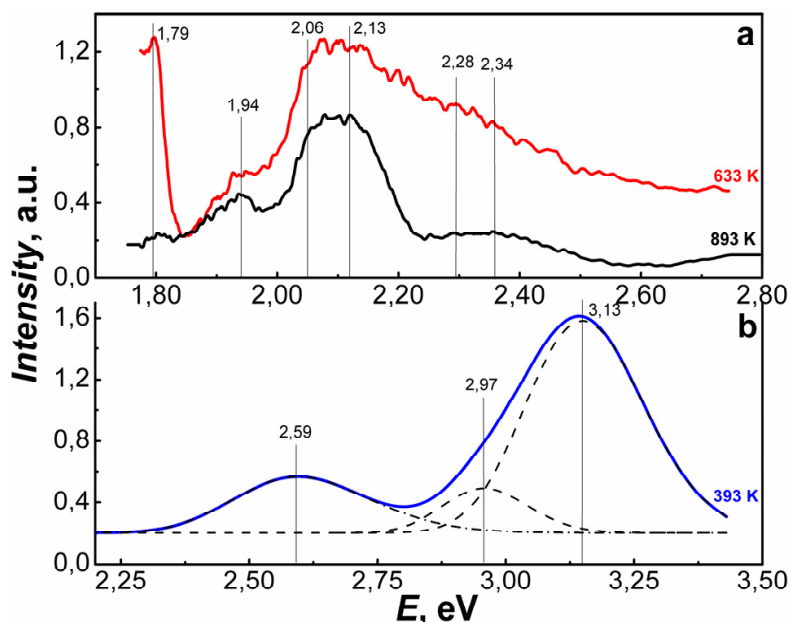

Figure 7. Typical PL spectra for ZnS films (a) and the example of the peak differentiation (b)

The investigations have shown that the Schottky defect V_{Zn} is a dominant defect type in ZnS films prepared at low substrate temperatures $T_s = (393-613)$ K. As T_s increases the number of single-charged Zn vacancies in the condensates decreases, and concentration of double-charged Zn vacancies increases. In the films deposited at higher substrate temperatures $T_s = (653-893)$ K single-charged S vacancies V_S^+ and double-charged S vacancies V_S^{2+} and interstitial Zn atoms Zn_i are dominating.

Such features of the PD ensemble in the samples are obviously caused by processes of condensation and re-evaporation of Zn and S atoms from the substrate. Actually, at low T_s the defect formation in the films is determined by higher S pressure comparing to Zn pressure in the mixture vapor providing Zn vacancy formation in ZnS condensates. As T_s increase the PD ensemble in the material is determined by the more rapid re-evaporation of the same S atoms from the substrate resulting in production of Zn-beneficiated films. Sulfur vacancies and interstitial Zn atoms are being dominant defects in such condensates.

T_s, K	Measurement range λ, nm	λ_1, nm E_1, eV	λ_2, nm E_2, eV	λ_3, nm E_3, eV	λ_4, nm E_4, eV	λ_5, nm E_5, eV	λ_6, nm E_6, eV	λ_7, nm E_7, eV	λ_8, nm E_8, eV
393	360÷640	**396**	417	478	-	-	603	-	-
		3.13	2.97	2.59	-	-	2.06	-	-
613	450÷720	-	-	**478**	-	-	603	640	-
		-	-	**2.59**	-	-	2.06	1.94	-
653	450÷720	-	-	-	530	**582**	**603**	640	**690**
		-	-	-	2.34	**2.13**	**2.06**	1.94	**1.79**
893	450÷720	-	-	-	530	**582**	**603**	640	690
		-	-	-	2.34	**2.13**	**2.06**	1.94	1.79
ΔE_i, eV Exper.	-	**0.55**	**0.71**	**1.09**	**1.34**	1.55 **1.40**	1.62 **1.40**	**1.74**	1.89 **1.74**
Defect	-	V_{Zn}^-	$O_s, V_{Zn}^{2-})S_i^-$	V_{Zn}^{2-}	Cu	V_S^{2+}	V_S^{2+}	V_S^+	V_S^+
ΔE_i, eV ref.	-	0.60	0.70	1.10	-	1.40	1.40	1.90	1.90
Reference data	-	[107]	[107, 108]	[104]	[104]	[104]	[104]	[104]	[104]

Table 8. Results of PL spectra working-out and their comparison with reference data (solid values are for peaks of maximum intensity)

The PL spectra of ZnS films have also revealed low intensity lines from the activator impurity (Cu) and, possible, S_i^- [106] or a complex defect (O_s, V_{Zn}^{2-}) [107]. Results of studying low-temperature PL allowed constructing energy position model of native point defects in zinc sulfide films prepared by quasi-closed space technique (Fig. 8).
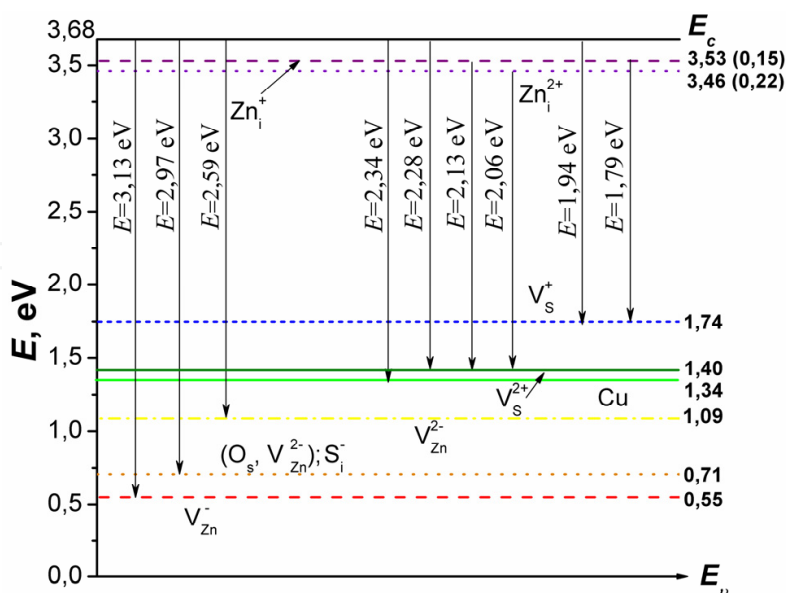

Figure 8. The model of the level positions for native point defects in band gap of ZnS films

To explain the experimental results we have used quasi-chemical formalism for modeling the point defects ensemble in the examined chalcogenide films in dependence on physical

technical conditions of layer condensation. This method concerns all defects, electrons and holes as components of thermodynamic equilibrium in the bulk crystal (complete equilibrium of the point defects). Then the modeling procedure reduces to solving set of equations which describe penetration of point defects into solid from the gas state along with the equation of electroneutrality and intrinsic conductivity equation [109-110]. The most complete spectrum of the native defects was taken into account under modeling the point defects ensemble. Calculations were carried out for the complete defects' equilibrium as well as for their quenching. Under modeling we have used energies of native defects formation obtained «*ab initio*» in [56-60]. Reference data of ionization energies of acceptor and donor centers of point defects in CdTe, ZnS, and ZnTe were used along with results of our experiments. Main data of modeling are presented in [111-116].

6. Conclusions

1. Express-method of IS providing maximum information on deep centers in high-resistive films based on analysis of SCLC CVC is developed and allows without additional studies
- identifying current mechanism in the structure as SCLC;
- receiving correct information on LS parameters in the gap of material: energy position, concentration and energy distribution immediately from the experimental CVCs without model framework.
2. Using IS method the LS spectrum in the gap of polycrystalline (and monocrystalline) films of II-VI compounds is examined. These results are checked and made more accurately by analysis of σ - T – functions and low-temperature luminescence.
3. Using the methods mentioned above in the gap of polycrystalline material are revealed the LS with following energy positions: $E_{t1} = 0.05$, $E_{t2} = (0.14 \div 0.15)$, $E_{t3} = (0.20 \div 0.21)$, $E_{t4} = (0.32 \div 0.34)$, $E_{t5} = (0.42 \div 0.43)$, $E_{t6} = (0.51 \div 0.52)$, $E_{t7} = (0.57 \div 0.58)$, $E_{t8} = (0.69 \div 0.70)$ eV (ZnTe); $E_{t1} = (0.13 \div 0.15)$, $E_{t2} = (0.39 \div 0.40)$, $E_{t3} = (0.45 \div 0.46)$, $E_{t4} = (0.51 \div 0.53)$, $E_{t5} = (0.56 \div 0.57)$, $E_{t6} = (0.60 \div 0.63)$, $E_{t7} = (0.68 \div 0.70)$ eV (CdTe); $E_{t1} = 0.03$, $E_{t2} = (0.07 \div 0.08)$, $E_{t3} = 0.15$, $E_{t4} = (0.23 \div 0.24)$, $E_{t5} = 0.33$, $E_{t6} = 0.46$, $E_{t7} = 0.87$, $E_{t8} = 1.94$, $E_{t9} = 2.34$, $E_{t10} = 2.59$, $E_{t11} = 2.97$, $E_{t12} = 3.13$ eV (ZnS) and concentration $N_t = (10^{19} – 10^{21})$ m^{-3}. Comparing reference data produced an identification of these levels as ones belonging to native point defects, uncontrolled impurities and their complexes. The wide range of LS revealed is due to high-sensitive methods used under investigations as well as because of examining traps in the intermediate layer of the films forming under condensation near the substrate.

Author details

Denys Kurbatov and Anatoliy Opanasyuk
Sumy State University, Sumy, Ukraine

Halyna Khlyap
TU Kaiserslautern, Kaiserslautern, Germany

Acknowledgement

7. References

[1] Georgobiani, A. (1974). Wide Band gap II-VI Semiconductors and Perspectives of Their Usage (in Russian), *Uspekhi Fizicheskikh Nauk*, Vol.113, No.1, pp. 129-155, ISSN 0042-1294.

[2] Pautrat, J. (1994). II–VI Semiconductor Microstructures: From Physics to Optoelectronics, *Journal de Physique III*, Vol.4, – pp. 2413-2425, ISSN 1155-4320.

[3] Takahashi, K., Yoshikawa, A. & Sandhu, A. (2007). *Wide Bandgap Semiconductors. Fundamental Properties and Modern Photonic and Electronic Devices*, Springer, ISBN, Berlin, Heidelberg, NewYork, Germany, USA.

[4] Owens, A. (2004). Compound Semiconductor Radiation Detectors, *Nuclear Instrumental Methods*, Vol. 531, pp. 18-37, ISSN 0168-9002.

[5] Grinev, B., Ryzhikov, V. & Seminozhenko, V. (2007). *Scintillation Detectors and Radiation Control Systems on Their Base (in Russian)*, Naukova Dumka, ISBN, Kyiv, Ukraine.

[6] Berchenko, N., Krevs, V. & Seredin, V. (1982). *Reference Tables (in Russian)*, Voenizdat, ISBN, Moskov, USSR.

[7] Ohring, M. (1992). *The Materials Science of Thin Films*, Academic Press, ISBN, NewYork, USA.

[8] Poortmans, J. & Arkhipov, V. (2006). *Thin Film Solar Cells: Fabrication, Characterization and Application*, John Wiley & Sons, Ltd. IMEC, ISBN, Leuven, Belgium.

[9] Panchekha, P. (2000). Structure and Technology Problems of II-VI Semiconductor Films, *Functional materials*, Vol.7, No.2, pp. 1-5, ISSN 1616-3028.

[10] Holt, D. & Yacobi, B. (2007). *Extended defects in semiconductors. Electronic properties, device effects and structures*, Cambridge University press, ISBN, New York, Melbourne, Madrid, Cape Town, USA, Australia, Spain, South Africa.

[11] Milns, A. (1977). *Impurities with Deep Levels in Semiconductors (in Russian)*, Mir, ISBN, Moskow, USSR.

[12] Shaskolskaya, M. (1984). *Crystallography: Studying Reference for Technical Universities (in Russian)*, Vysshaya Shkola, ISBN, Moskow, USSR.

[13] Korbutyak, D. & Melnychuk, S. (2000). *Cadmium Telluride: Impurity-Defect States and Detector Properties*, Ivan Fedorov, ISBN, Kyiv, Ukraine.

[14] Fochuk, P. (Experimental identification of the Point Defects/ P. Fochuk, O. Panchuk // CdTe and related Compounds: Physics, Defects, Hetero- and Nano-Structure, Crystal

growth, Surfaces and Applications. [R. Triboulet, P.Siffert]. Netherlands: Elsevier, 2010. – P. 292-362.

[15] Stokman, F. (1973) On the Classification of Traps and Recombination Centres, *Physica Status Solidi A*, Vol.20. – pp. 217-220, ISSN 1862-6319.

[16] Serdyuk, V., Chemeresyuk, G. & Terek, M. (1982). *Photoelectric Processes in Semiconductors*, Vyshcha Shkola, Main Edition, ISBN, Odessa, USSR.

[17] Meyer, B. & Stadler, W. (1996). Native Defect Identification in II-VI Materials, *Journal of Crystal Growth*, Vol.161, pp. 119-127, ISSN 0022-0248.

[18] Neumark, G. (1997). Defects in Wide Band Gap II-VI Crystals, *Material Science and Engineering A*, Vol.R21, No.1, - pp. 1-46, ISSN 0921-5093.

[19] Grundmann, M. (2010). *The Physics of Semiconductors. An Introduction Including Nanophysics and Applications*, Springer-Verlag, ISBN, Berlin, Heidelberg, Germany.

[20] Kosyak, V., Opanasyuk, A. & Panchal, J. (2011). Structural and Substructural Properties of the Zinc and Cadmium Chalcogenides (review), *Journal of Nano and Electronic Physics*, Vol.3, No.1, – pp. 274-301, ISSN 2077-6772.

[21] Pavlov, A. (1987). *Methods of Measuring the Semiconductor Materials Parameters (in Russian)*, Vysshaya Shkola, ISBN, Moskow, USSR.

[22] Vorobjev, Ju., Dobropolskiy, V. & Strikha, V. (1988). *Methods of Semiconductors Investigation*, Vyshcha Shkola, ISBN, Kyiv, USSR.

[23] Gorokhovatskij, Ju. & Bordovskij, G. (1991). *Thermoactivation Current Spectroscopy of High-ohmic Semiconductors and Dielectrics*, Nauka, ISBN, Moskow, USSR.

[24] Lampert, M. & Mark, P. (1973). *Injection Currents in Solid States*, Mir, ISBN, Moskow, USSR.

[25] Kao, K. (1984). *Electrons Transport in Solid States.* Vol.1, Mir, ISBN, Moskow, USSR.

[26] Lalitha, S., Sathyamoorthy, R. & Senthilarasu, S. (2004). Characterization of CdTe Thin Film-dependence of Structural and Optical Properties on Temperature and Thickness, *Solar Energy Materials & Solar Cells*, Vol.82, – pp. 187-199, ISSN 0927-0248.

[27] Ibrahim, A. (2006). DC Electrical Conduction of Zinc Telluride Thin Films, *Vacuum*, Vol.81, pp. 527–530, ISSN.

[28] Rose, A. (1955). Recombination Processes in Insulators and Semiconductors, *Physical Review*, Vol.97, pp. 322—323, ISSN 1943-2879.

[29] Rose A. (1955). Space–charge–limited Currents in Solids, *Physical Review*, Vol.97, pp. 1538–1544, ISSN 1943-2879

[30] Nespurek, S. & Sworakowsky, J. (1980). Evolution of Validity of Analytical Equations Describing Steady–state Space–charge–limited Current–voltage–characteristics, *Czechoslovak Journal of Physics*, Vol.B30, No.10, pp. 1148–1156, ISSN 0011-4626.

[31] Mark, P. & Helfrich, W. (1962). Space–charge–limited Currents in Organic Crystals, *Journal of Applied Physics*, Vol.33, pp. 205–215, ISSN 0021-8979.

[32] Thomas, J., Williams, J. & Turton L. (1968). Lattice Imperfections in Organic Solids. Part 3, 4, *Transactions of the Faraday Society*, Vol.64, pp. 2496—2504, ISSN 0014-7672.

[33] Hwang, W. & Kao, K. (1976). Studies of the Theory of Single and Double Injections in Solids with a Gaussian Trap Distribution, *Solid State Electronics*, Vol.19, pp. 1045–1047, ISSN 0038-1101.

[34] Nespurec, S. & Semejtec, P. (1972). Space Charge Limited Currents in Insulators With Gaussian Distribution of Traps, *Czechoslovak Journal of Physics*, Vol.B22, pp. 160–175, ISSN 0011-4626.

[35] Boncham, J. (1973). SCLC Theory for a Gaussian Trap Distribution, *Australian Journal of Chemistry*, Vol.26, pp. 927–939, ISSN 0004-9425.

[36] Simmons, J. & Tarn, M. (1973). Theory of Isothermal Currents and the Direct Determination of Trap Parameters in Semiconductors and Insulators Containing Arbitrary Trap Distributions, *Physical Review*, Vol.B7, pp. 3706-3713, ISSN 1943-2879.

[37] Pfister, J. (1974). Note of Interpretation of Space–charge–limited Currents With Traps, *Physica Status Solidi A*, Vol.24, No.1, pp. K15-K17, ISSN 1862-6319.

[38] Manfredotti, C., de Blasi, C. & Galassini, S. (1976). Analysis of SCLC Curves by a New Direct Method , *Physica Status Solidi A*, Vol.36, No.2, pp. 569-577, ISSN 1862-6319.

[39] Nespurek, S. & Sworakowski, J. (1978). A Differential Method of Analysis of Steady-state Space-charge-limited Currents: an Extension, *Physica Status Solidi A.*, Vol.49, pp. 149-152, ISSN 1862-6319.

[40] Nespurek, S. & Sworakowski, J. (1980). Use of Space–charge–limited Current Measurement to Determine of Properties of Energetic Distributions of Bulk Traps, *Journal of Applied Physics*, Vol.51, No.4, pp. 2098-2102, ISSN 0021-8979.

[41] Nespurek, S. & Sworakowski, J. (1990). Spectroscopy of Local States in Molecular Materials Using Space-charge-limited Currents, *Radiation Physics and Chemistry*, Vol.36, No.1, pp. 3-12, ISSN 0969-806X.

[42] Nespurec, S., Obrda, J. & Sworakowsky, J. (1978). Study of Traps for Current Carriers in Organic Solids N,N' – Diphenyl–p–Phenylenediamine, *Physica Status Solidi A*, Vol.46, No.1, pp. 273–280, ISSN 1862-6319.

[43] Lyubchak, V., Opanasyuk, A. & Tyrkusova, N. (1999). Injection Spectroscopy Method for investigation of Deep Centers in Cadmium Telluride Films (in Ukrainian), *Ukrayinskyi Fizychnyi Zhurnal*, Vol.44, No.6, pp. 741-747, ISSN 0503-1265.

[44] Opanasyuk, A., Tyrkusova, N. & Protsenko, I. (2000). Some Features of the Distributions Deep States Reconstruction by Injection Spectroscopy Method (in Ukrainian), *Zhurnal Fizychnykh Doslidzhen*, Vol.4, No.2, pp. 208-215, ISSN 1027-4642.

[45] Opanasyuk, A., Opanasyuk, N. & Tyrkusova, N. (2003), High-temperature Injection Spectroscopy of Deep Traps in CdTe Polycrystalline Films, *Semiconductor Physics, Quantum Electronics & Optoelectronics*, Vol.6, No.4, pp. 444-449, ISSN 1560-8034.

[46] Tikhonov, A. & Jagola, A. (1990). *Numerical Nethods of Non-correct Problems Solution*, Nauka, ISBN, Moskow, USSR..

[47] Zavjalov, Ju., Kvasov, B. & Miroshnichenko, V. (1980). *Spline-functions Methods*, Nauka, ISBN, Moskow, USSR..

[48] Turkusova, N. (2002). *Injection Spectroscopy of Deep Trap Levels in Cadmium Telluride Films, PhD Thesis (in Ukrainian)*, Sumy State University, Sumy, Ukraine.

[49] Kosyak, V., Opanasyuk, A. & Bukivskij, P. (2010). Study of the Structural and Photoluminescence Properties of CdTe Polycrystalline Films Deposited by Closed Space Vacuum Sublimation, *Journal of Crystal Growth*, Vol.312, pp. 1726-1730, ISSN 0022-0248.

[50] Kurbatov, D., Khlyap, H. & Opanasyuk, A. (2009). Substrate–temperature Effect on the Microstructural and Optical Properties of ZnS Films Obtained by Close–spaced Vacuum Sublimation, *Physica Status Solidi A*, Vol.206, No.7, pp. 1549-1557, ISSN 1862-6319.

[51] (1988). *Selected Powder Diffraction Data for Education Straining (Search Manual and Data Cards)*, International Centre for Diffraction Data, USA.

[52] Zjuganov, A. & Svechnikov, S. (1981). *Injection-contact Effects in Semiconductors (in Russian)*, Naukova Dumka, ISBN, Kiev, USSR.

[53] Zjuganov, A., Smertenko, P. & Shulga, E. (1979). Generalized Method of Determination the Volume and Contact Semiconductor Parameters by Current-voltage characteristic (in Russian), *Poluprovodnikovaja Tekhnika i Elektronika*, Vol.29, pp.48-54, ISSN.

[54] Kurbatov, D., Kolesnyk, M. & Opanasyuk, A. (2009). The Substructural and Optical Characteristics of ZnTe Thin Films, *Semiconductor Physics, Quantum Electronics & Optoelectronics*, Vol.12, No.1, pp. 35-40, ISSN 1560-8034.

[55] Kurbatov, D., Denisenko, V. & Opanasyuk, A. (2008). Investigations of Surface Morphology and Chemical Composition Ag/ZnS/Glassceramic Thin Films Structure, *Semiconductor Physics, Quantum Electronics & Optoelectronics*, Vol.11, No.4, pp. 252-256, ISSN 1560-8034.

[56] Balogh, A., Duvanov, D. & Kurbatov, D. (2008). Rutherford Backscattering and X–ray Diffraction Analysis of Ag/ZnS/Glass Multilayer System, *Photoelectronics*, Vol.B.17, pp.140-143, ISSN 0235-2435.

[57] Wei, S. & Znang, S. (2002). Chemical Trends of Defect Formation and Doping Limit in II–VI Semiconductor: The Case of CdTe, *Physical Review B*, Vol.66, pp. 1-10, ISSN 0163-1829.

[58] Wei, S. & Zhang, S. (2002). First-Principles Study of Doping Limits of CdTe, *Physica Status Solidi B*, Vol.229, No. 1, pp. 305–310, ISSN 0370-1972.

[59] Soundararajan, R., lynn, K. & Awadallah, S. (2006). Study of Defect Levels in CdTe Using Thermoelectric Effect Spectroscopy, *Journal of Electronic Materials*, Vol.35, No.6, pp., ISSN 0361-5235.

[60] Berding, M. (1999). Native Defects in CdTe, *Physical Review B*, Vol.60, No.12, pp. 8943-8950, ISSN 0163-1829.

[61] Berding M. (1999). Annealing Conditions for Intrinsic CdTe, *Applied Physics Letters*, Vol.74, No.4, pp. 552-554, ISSN 0003-6951.

[62] X.Mathew. Photo-induced current transient spectroscopic studu of the traps in *CdTe// Solar Energy Materials & Solar Cells*. 76, pp. 225-242 (2003).

[63] Mahalingam, T., John, V. & Ravi, G. (2002). Microstructural Characterization of Electrosynthesized ZnTe Thin films, *Crystal Research and Technology*, Vol.37, No.4, pp. 329–339, ISSN 1521-4079.

[64] Ibrahim, A, El-Sayed, N. & Kaid, M. (2004). Structural and Electrical Properties of Evaporated ZnTe Thin Films, *Vacuum*, Vol.75, pp. 189–194, ISSN 0042-207X.

[65] Dean, P., Venghaus, H. & Pfister, J. (1978). The Nature of the Predominant Acceptors in High Quality Zinc Telluride, *Journal of Luminescence*, Vol.16, pp. 363-394, ISSN 0022-2313.

[66] Bhunia, S., Pal, D. & Bose, N. (1998). Photoluminescence and Photoconductivity in Hydrogen–passivated ZnTe, *Semiconductor Science and Technology*, Vol.13, pp. 1434-1438, ISSN 0268-1242.

[67] Sadofjev, Ju. & Gorshkov, M. (2002). Deep Level Spectra in ZnTe:Cr^{2+} Layers Obtained by Epitaxy from Molecular Beams (in Russian), *Fizika I Tekhnika Poluprovodnikov*, Vol.36, No.5, pp. 525-527, ISSN 0015-3222.

[68] Korbutyak, D., Vakhnyak, N. & Tsutsura, D. (2007). Investigation of Photoluminescence and Electroconductivity of ZnTe Grown in Hydrogen Atmosphere, *Ukrainian Journal of Physics*, Vol.52, No.4, pp. 378-381, ISSN 2071-0186.

[69] Feng, L., Mao, D. & Tang, J. (1996). The Structural, Optical, and Electrical Properties of Vacuum Evaporated Cu-doped ZnTe Polycrystalline Thin Films, *Journal of Electronic Materials*, Vol. 25, pp. 1422–1427, ISSN 0361-5235.

[70] Atakova, M., Ramazanov, P. &Salman, E. (1973). Local Levels in a Zinc Sulfide Film, *Izvestiya Vysshikh Uchebnykh Zavedenii, Fizika*, Vol.10, pp. 95 – 98, ISSN 0021-3411.

[71] Venkata Subbaiah Y., Prathap, P. & Ramakrishna Reddy, K. (2006). Structural, Electrical and Optical Properties of ZnS Films Deposited by Close-spaced Evaporation, *Applied Surface Science*, Vol. 253, pp. 2409 – 2415, ISSN 0169-4332.

[72] Venkata Subbaiah, Y., Prathap, P. & Ramakrishna Reddy, K. (2008). Thickness Effect on the Microstructure, Morphology and Optoelectronic Properties of ZnS Films, *Journal of Physics: Condensed Materials*, Vol.20, pp. 035205 – 035215, ISSN 0953-8984.

[73] Turan, E., Zor, M. & Aybek, A. (2007). Thermally Stimulated Currents in ZnS Sandwich Structure Deposited by Spray Pyrolysis, *Physica B: Condensed Materials*, Vol.395, No.1, pp. 57 – 64, ISSN 0921-4526.

[74] Abbas, J., Mehta, C. & Saini, G. (2007). Preparation and Characterization of n-ZnS and its Self-assembled Thin Film, *Digest Journal of Nanomaterials and Biostructures*, Vol.2, No.3, pp. 271 – 276, ISSN 1842-3582.

[75] Kvit, A., Medvedev, S. & Klevkov, Ju. (1998). Optical Spectroscopy of Deep States in ZnTe (in Russian), *Fizika I Tekhnika Poluprovodnikov*, Vol.40, No.6, pp. 1010-1017, ISSN 0015-3222.

[76] Bagaev, V., Zajtsev, V. & Klevkov, Ju. (2003). Influence of Annealing in Vapors and in Liquid Zn on ZnTe High-frequency Polycrustalline Photoluminescence (in Russian), *Fizika I Tekhnika Poluprovodnikov*, Vol.37, No.3, pp. 299-303, ISSN 0015-3222.

[77] Klevkov, Ju., Martovitskij, V., Bagaev, V. (2006). Morphology, Twins Formation and Photoluminescence of ZnTe crystals Grown by Chemical Synthesis of Components From Vapor Phase (in Russian), *Fizika I Tekhnika Poluprovodnikov*, Vol.40, No.2, pp. 153-159, ISSN 0015-3222.

[78] Klevkov, Ju., Kolosov, S. & Krivobokov, V. (2008). Electrical Properties, Photoconductivity and Photoluminescence of large-crystalline p-CdTe (in Russian), *Fizika I Tekhnika Poluprovodnikov*, Vol.42, No.11, pp. 1291-1296, ISSN 0015-3222.

[79] Bagaev, V., Klevkov, Ju. & Krivobokov, V. (2008). Photoluminescence Spectrum Change Near the Twins Boundaries in ZnTe Crystals Obtained by High-speed Crystallization (in Russian), *Fizika Tverdogo Tela*, V.50, No.5, pp. 774-780, ISSN 0042-1294.

[80] Makhniy V. & Gryvun, V. (2006). Diffusion ZnTe:Sn Layers with Electron Conductivity (in Russian), *Fizika I Tekhnika Poluprovodnikov*, Vol.40, No.7, pp. 794-795, ISSN 0015-3222.

[81] Tsutsura, D., Korbutyak, O. & Pihur, O. (2007). On Interaction of Hydrogen Atoms With Complex Defects in CdTe and ZnTe, *Ukrainian Journal of Physics*, Vol.52, No.12, pp. 1165-1169, ISSN 2071-0186.

[82] Taguchi, T, Fujita, S. & Inushi, Y. (1978). Growth of High-purity ZnTe Single Crystals by the Sublimation Travelling Heater Method, *Journal of Crystal Growth*, Vol.45, pp. 204-213, ISSN 0022-0248.

[83] Dean, P. (1979). Copper, the Dominant Acceptor in Refined, Undoped Zinc Telluride, *Luminescence*, Vol.21, pp. 75-83, ISSN 1522-7243.

[84] Garcia, J., Remon, A. & Munoz, V. (2000). Annealing-induced Changes in the Electronic and Structural Properties of ZnTe Substrates, *Journal of Materials Research*, Vol.15, No.7, pp. 1612-1616, ISSN 0884-2914.

[85] Uen, W., Chou, S. & Shin, H. (2004), Characterizations of ZnTe Bulks Grown by Temperature Gradient Solution Growth, *Materials Science & Engineering A*, Vol.B106, pp. 27-32, ISSN 0921-5093.

[86] Yoshino, K, Yoneta, V. & Onmori, K. (2004). Annealing Effects of High–quality ZnTe Substrate, *Journal of Electronic Materials*, Vol.33, No.6, pp. 579-582, ISSN 0361-5235.

[87] Yoshino, K., Kakeno, T. & Yoneta, M. (2005). Annealing Effects of High–quality ZnTe Substrate, *Journal of Material Science: Materials in Electronics*, Vol.16, pp. 445-448, ISSN.0957-4522.

[88] Ichiba, A., Ueno, J. & Ogura, K. (2006). Growth and Optical Property Characterizations of ZnTe:(Al, N) layers Using Two Co–doping Techniques, *Physica Status Solidi C*, Vol.3, No.4, pp. 789-792, ISSN 1610-1642.

[89] Bose, D. & Bhunia, S. (2005). High Resistivity In–doped ZnTe: Electrical and Optical Properties, *Bulletin of Material Science*, Vol.28, No.7, pp. 647-650, ISSN 0250-4707.

[90] Grill, R., Franc, J, & Turkevych, I. (2002). Defect-induced Optical Transitions in CdTe and $Cd_{0,96}Zn_{0,04}Te$ *Semiconductor Science and Technology*, Vol.17, pp. 1282-1287, ISSN 0268-1242.

[91] Ushakov, V. & Klevkov, Ju. (2007). Microphotoluminescence of Undoped Cadmium Telluride Obtained by Non-equilibrium Method of Direct Synthesis in Components Fluctuation (in Russian), *Fizika I Tekhnika Poluprovodnikov*, Vol.41, No.2, pp. 140-143, ISSN 0015-3222.

[92] Babentsov, V., Corregidor, V. & Castano, J. (2001). Compensation of CdTe by Doping With Gallium, *Crystal Research and Technology*, Vol.36, No.6, pp. 535-542, ISSN 1521-4079.

[93] Tarbayev, G. & Shepelskij. (2006). Two Series of "Dislocation" Photoluminescence Lines in Cadmium Telluride Crystals (in Russian), *Fizika I Tekhnika Poluprovodnikov*, Vol.40, No.10, pp. 1175-1180, ISSN 0015-3222.

[94] Aguilar-Hernandez, J., Contreras-Puente, J. & Vidal-Larramendi J. (2003). Influence of the Growth Conditions on the Photoluminescence Spectrum of CdTe Polycrystalline Films Deposited by the Close Space Vapor Transport Technique, *Thin Solid Films*, Vol.426, pp. 132-134, ISSN 0040-6090.

[95] Aguilar-Hernandez, J., Cardenas-Garcia, M. & Contreras-Puente, G. (2003). Analysis of the 1,55 eV PL Band of CdTe Polycrystalline Films, *Material Science & Engineering A*, Vol.B102, pp. 203-206, ISSN 0921-5093.

[96] Armani, N., Ferrari, C. & Salviati, G. (2002). Defect-induced Luminescence in High–resistivity High–purity Undoped CdTe Crystals, *Journal of Physics: Condensed Matterials*, Vol.14, pp. 13203-13209, ISSN 0953-8984.

[97] Gheluwe, J., Versluys, J. & Poelman, D. (2005). Photoluminescence Study of Polycrystalline CdS/CdTe Thin Film Solar Cells, *Thin Solid Films*,Vol.480–481, pp. 264-268, ISSN 0040-6090.

[98] Okamoto, T., Yamada, A. & Konagai, M. (2001). Optical and Electrical Characterizations of Highly Efficient CdTe Thin Film Solar Cells, *Thin Solid Films*, Vol.387, pp. 6-10, ISSN 0040-6090.

[99] Holliday, D., Potter, M. & Boyle, D. (2001). Photoluminescence Characterisation of Ion Implanted CdTe, *Material Research Society, Symposium Proceedings*, Vol.668, pp. H1.8.1-H1.8.6, ISSN 0272-9172.

[100] Palosz, W., Grasza, K. & Boyd, P. (2003). Photoluminescence of CdTe Crystals Grown Physical Vapor Transport, *Journal of Electronic Materials*, Vol.32, No.7, pp.747-751, ISSN 0361-5235.

[101] Corregidor, V., Saucedo, E. & Fornaro, L. (2002). Defects in CdTe Polycrystalline Films Grown by Physical Vapour Deposition, *Materials Science and Engineering A*, Vol.B 91–92, pp. 525-528, ISSN 0921-5093.

[102] Soundararajan, R., Lynn, K. & Awadallah, S. (2006). Study of Defect Levels in CdTe Using Thermoelectric Effect Spectroscopy, *Journal of Electronic Materials*, Vol.35, No.6, pp. 1333-1340, ISSN 0361-5235.

[103] Babentsov, V. & Tarbaev. (1998). Photoluminescence of Re-crystallized by Nano-second Laser Irradiation Cadmium Telluride (in Russian), *Fizika I Tekhnika Poluprovodnikov*, Vol.32, No.1, pp. 32-35, ISSN 0015-3222.

[104] Morozova, N. & Kuznetsov, V. (1987). *Zinc Sulfide. Obtaining and Optical Properties (in Russian)*, Nauka, ISBN, Moskow, USSR.

[105] Sahraei, R., Aval, J. & Goudarzi, A. (2008). Compositional, Structural and Optical Study of Nanocrystalline ZnS Thin Films Prepared by a New Chemical Bath Deposition Route, *Journal of Alloys and Compounds*, Vol.466, pp. 488-492, ISSN 0925-8388.

[106] Prathap, P. Revathi, N. & Venkata Subbaiah, Y. (2008). Thickness Effect on the Microstructure, Morphology and Optoelectronic Properties of ZnS Films, *Journal of Physics: Condensed Materials*, Vol.20, pp. 035205-035215, ISSN 0953-8984.

[107] Prathap, P. & Venkata Subbaiah, Y. (2007). Influence of Growth Rate on Microstructure and Optoelectronic Behaviour of ZnS Films, *Journal of Physics D: Applied Physics*, Vol. 40, pp. 5275-5282, ISSN 0022-3727.

[108] Lee, H. & Lee, S. (2007). Deposition and Optical Properties of Nanocrystalline ZnS Thin Films by a Chemical Method , *Current Applied Physics*, Vol.7, pp. 193-197, ISSN 1567-1739.

[109] Kroger, F. (1964). *The chemistry of Imperfect Crystals*, North-holland publishing company, ISBN, Amsterdam, Netherlands.

[110] Grill, R. & Zappetini, A. (2004). Point Defects and Diffusion in Cadmium Telluride, *Progress in Crystal Growth and Characterization of Materials*, Vol.48, pp .209-244, ISSN 0146-3535.

[111] Kosyak, V. & Opanasyuk, A. (2005). Point Defects Encemble in CdTe Single Crystals in the Case of full Equilibrium and Quenching (in Ukrainian), *Fizyka I Himiya Tverdych Til*, Vol.6, No.3, pp. 461-471, ISSN 1729-4428.

[112] Kosyak, V., Opanasyuk, A. & Protsenko, I. (2005). Ensemble of Point Defects in Single Crystals and Films in the Case of Full Equilibrium and Quenching, *Functional Materials*, Vol.12, No.4, pp. 797-806, ISSN 1616-3028.

[113] Kosyak, V. & Opanasyuk, A. (2007). Calculation of Fermi Level Location and Point Defect Ensemble in CdTe Single Crystal and Thin Films, *Semiconductor Physics, Quantum Electronics & Optoelectronics*, Vol.10, No.3, pp. 95-102, ISSN 1560-8034.

[114] Kolesnik, M., Kosyak, V. & Opanasyuk, A. (2007). Calculation of Point Defects Ensemble in CdTe Films Considering Transport Phenomenon in Gas Phase, *Radiation Measurements*, Vol.42, No.4–5, pp. 855-858, ISSN 1350-4487.

[115] Kosyak, V., Kolesnik, M. & Opanasyuk, A. (2008). Point Defect Structure in CdTe and ZnTe Thin Films, *Journal of Material Science: Materials in Electronics*, Vol.19, No.1, pp. S375-S381, ISSN 0957-4522.

[116] Kurbatov, D, Kosyak, V., Opanasyuk, A. (2009). Native Point Defects in ZnS Films, *Physica. B. Condensed Materials*, Vol.404, No.23–24, pp. 5002-5005, ISSN 0921-4526.